RESEARCH ARTICLE

Gene-transcription factor regulatory networks implicate primary cilia in the evolution of vertebrate sex determination and expand models of epigenetic regulation

Thea B. Gessler[1,2*], **Dean C. Adams**[1], **Nicole Valenzuela**[1*]

1 Department of Ecology, Evolution, and Organismal Biology, Iowa State University, Ames, Iowa, United States of America, **2** Genetics and Genomics Program, Iowa State University, Ames, Iowa, United States of America

* thea.gessler@gmail.com (TBG), nvalenzu@iastate.edu (NV)

Check for updates

OPEN ACCESS

Citation: Gessler TB, Adams DC, Valenzuela N (2026) Gene-transcription factor regulatory networks implicate primary cilia in the evolution of vertebrate sex determination and expand models of epigenetic regulation. PLoS One 21(7): e0353280. https://doi.org/10.1371/journal.pone.0353280

Editor: Christoph Englert, Leibniz Institute on Aging - Fritz Lipmann Institute (FLI), GERMANY

Received: February 21, 2026

Accepted: June 22, 2026

Published: July 29, 2026

Copyright: © 2026 Gessler et al. This is an open access article distributed under the terms of the Creative Commons Attribution License, which permits unrestricted use, distribution, and reproduction in any medium, provided the original author and source are credited.

Data availability statement: No new data were generated for this paper but have been previously published; however sequencing reads are available in the Short Read Archive at NCBI: BioProjects PRJNA683586 (Apalone spinifera embryos—SRR13224849-SRR13224888)

Abstract

The molecular architecture underlying diverse vertebrate sex-determining systems remains elusive despite fragmentary evidence of changes in upstream regulators and downstream mediators. Here we modeled species-specific regulatory networks of urogonadal development for turtles with contrasting mechanisms [*Apalone spinifera* – ZZ/ZW genotypic sex determination (GSD), and *Chrysemys picta* – temperature-dependent sex determination (TSD)] using matched data from time-course sampling. We uncovered key steps in the evolutionary transition of sex determination by testing for conservation or divergence of network modular components. Specifically, we tested these alternative hypotheses: first, transcription factor (TF) hubs and their target genes are conserved between species (null H0); second, the same TF hub acquired a new set of target genes in a species, retaining or not ancestral functions (H1 and variants); third, a new TF hub took over the regulation of the former gene targets of an ancestral TF (H2); and finally, complete overhaul occured where both ancestral TF hubs and their target genes were replaced in a species (H3). Results implicate primary cilia as integrators of environmental signals underlying TSD, because known thermosensitive TSD components (e.g., calcium-redox, pSTAT3, *Wnt*/*Rspo1*/*β-catenin*, *Dhh*) overrepresented in our results are linked to primary cilia. TFs that evolved between species also regulate primary cilia and point to key changes in their sensory machinery that accompanied TSD-GSD transitions (e.g., calcium/ion channels or membrane transport components in *Chrysemys* versus structural elements and ciliogenesis in *Apalone*). This novel Primary Cilia Integration hypothesis expands current models of epigenetic regulation of turtle sexual development, the evolution of plasticity versus canalization, and warrants functional validation.

and PRJNA594037 (Chrysemys picta embryos—study number SRP237291; SRR10674595-SRR10674614).

Funding: This work was funded in part by US National Science Foundation grants IOS 1555999 and IOS 2127995 to NV. The research reported in this paper is partially supported by the HPC@ISU equipment at Iowa State University, some of which has been purchased through funding provided by the US National Science Foundation under MRI grants number 1726447 and 2018594. All opinions, findings, and conclusions expressed in this paper are those of the authors.

Competing interests: The authors have declared that no competing interests exist.

Abbreviations: CaRe, calcium redox; DAG, directed acyclic graph; ESD, environmental sex determination; FPT, female producing temperature; GRN, gene regulatory network; GSD, genotypic sex determination; MPT, male producing temperature; Mya, million years ago; PC, principal components; ROS, reactive oxygen species; SDM, sex determination mechanism; TF, transcription factor; TFBS, transcription factor binding site; TSD, temperature-dependent sex determination.

Introduction

Vertebrate sex determination provides a compelling example of a developmental mechanism that diverges greatly despite sharing highly conserved gene players [1–4], a case of developmental systems drift [5]. Specifically, vertebrate sex-determining mechanisms (SDMs) span a spectrum from fairly strict environmental sex determination (ESD) to strongly canalized genotypic sex determination (GSD) [6,7]. SDMs are governed by genes recycled frequently among taxa, but their position or regulation in the network is shuffled repeatedly by evolution, such as occurred for *Dmrt1* [8–10], *Sox9* [11], and *Aromatase* [12], among many others. Importantly, our full understanding of the rewiring of the genetic network underlying the diversity of vertebrate SDMs is obscured in part because much of our knowledge still relies on mouse and human models [3].

Turtles are a vertebrate group particularly suited to unravel developmental network divergence as they showcase temperature-dependent sex determination (TSD)—a type of ESD, plus XX/XY and ZZ/ZW sex chromosomal systems of GSD [13]. These systems evolved independently multiple times, accompanied by accelerated molecular evolution of sexual development genes [14–16]. These natural experiments enable comparative analyses between closely related lineages with and without plastic sexual development to uncover the shifts in molecular architecture underlying these transitions [15,17] aided by growing 'omic resources in turtles [18–20]. Active research is devoted to identifying the elusive environmental sensor(s) that distinguishes TSD from GSD. Recent potential candidates include calcium and redox (CaRe) status sensors [21], and epigenetic histone modifications driving the temperature-specific activation or repression of *Dmrt1* [9,22], a masculinizing gene also implicated in a GSD turtle [23]. However, broader changes have accrued between TSD and GSD networks beyond these few candidate elements. Comparisons across turtles and other vertebrates revealed that transcriptional heterochrony contributes to the divergence in SDMs [1,6,24,25], such that agnostic genome-wide investigations should substantially illuminate these evolutionary events more broadly.

Divergence of developmental programs underlying phenotypic evolution often involve the evolution of gene regulatory network (GRN) components, such as cis-regulatory elements (CREs) that change the interaction between transcription factors (TFs) and the genes they regulate [26]. This is true for GRNs controlling animal sexual development, which at a broad taxonomic scale appear quite evolutionarily labile at the upstream trigger and more conserved in the downstream TFs [27]. TFs may regulate a multitude of genes in a GRN, acting as TF hubs, and may have pleiotropic effects in multiple biological processes. Thus, because changes in hubs can lead to profound phenotypic changes with potentially detrimental fitness effects [26], highly connected and central hubs are expected to evolve at a slower rate than peripheral elements of the GRN [28] (although adaptive evolution via changes to central hubs may be possible [28,29]), whereas changes can accumulate more gradually via shifts in gene target identity [26].

Here we constructed and compared gene-transcription factor interaction networks for two turtle species with contrasting SDMs: the painted turtle *Chrysemys picta*, a

TSD representative, and the spiny softshell turtle *Apalone spinifera*, a GSD species with an evolutionarily derived ZZ/ZW mechanism [16,30,31]. Species will be referred to by their genus name hereafter. This approach allowed us to build novel models about the molecular circuitry of TSD and GSD, test their predictions of how this circuitry evolved in these distinct lineages, and identify candidate elements for a putative role as key TSD or GSD regulators. Results indicate the involvement of primary cilia in the regulation and evolution of vertebrate sex determination. Primary cilia are organelles that nearly all cell types use to sense the context of cues from the external environment or internal signaling pathways [32]. Specifically, we tested the following non-mutually exclusive hypotheses about evolutionary patterns of turtle sexual development networks, by examining differences between species in TF hubs (i.e., TFs regulating many genes in the network), their target genes (Fig 1), and shifts in the associated functional annotations of candidate genes that would suggest a potential change in their regulatory role (i.e., a putative change in function). Of note, we use the terms hub and

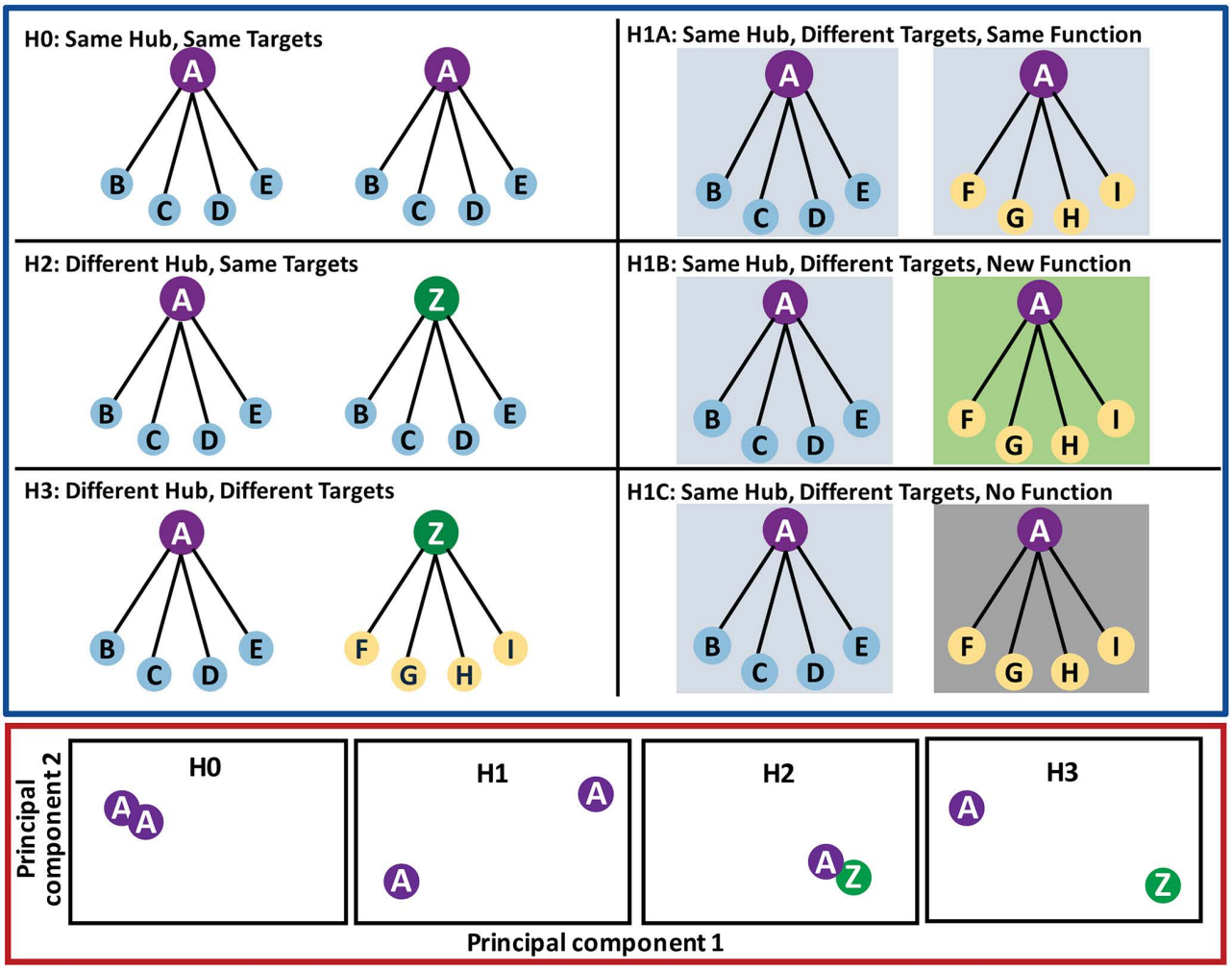


Fig 1. Illustration of predictions from the hypotheses of the evolution of vertebrate sex determination by shifts in the interactions of transcription factors and their predicted target genes. Top three rows encircled in blue: (H0) null hypothesis, i.e., network/module conservation, (H1) upstream conservation, downstream divergence, (H2) upstream divergence, downstream conservation, and (H3) full network/module overhaul. Bottom row encircled in red: depiction of the pattern of TF clustering in regulome space (i.e., principal components plot capturing differences in targeting patterns of TF hubs) expected under hypotheses H0, H1, H2, and H3 (see text for details).

https://doi.org/10.1371/journal.pone.0353280.g001

TF interchangeably, as the TFs examined here act as hubs within the subnetworks of the genes they target (the focus of much of our comparisons), while recognizing that in the context of broader networks some TFs may be more interconnected (i.e., hub-like) than others:

H0: Same hub, same targets hypothesis Neither the hub TFs nor their target genes vary between species. If this null hypothesis is supported, it would indicate evolutionary conservation of the network wiring between TSD and GSD. Partial support of this hypothesis for only some TFs would expose network connections under strong stabilizing selection. In contrast, such a finding for the entire network would be surprising given that these taxa split 175 Mya (timetree.org) and *Apalone*'s softshell turtle family shifted from TSD to GSD [31].

H1A: Same hub directs same function with new targets A conserved TF hub recruits a novel set of target genes that take over the regulation of the ancestral function. Support for H1A would uncover TFs subject to developmental systems drift [5] because the TF continues to direct the same function (determined by finding a conserved functional annotation of the targets in an overrepresentation test), but the gene targets implementing that function have changed between species.

H1B: Same hub directs different function with new targets: A conserved TF hub recruits a novel set of target genes, and these targets regulate a new function. Such a change could occur *via* natural selection for a new function via the rewiring of the TF's target genes (in which case an overrepresentation test would reveal species-specific functional annotations for each set of gene targets).

H1C: Same hub, new targets with no function: The TF hub remains conserved, but it regulates new target genes that have no detectable functional annotation as determined via overrepresentation tests (i.e., potential pseudofunctionalization). This pattern could result from genetic drift, perhaps when the original function regulated by a TF is released from selection by changes elsewhere in the network, facilitating gains or losses of TF binding sites (TFBSs) irrespective of their functional potential.

H2: New hub, same targets. A new TF hub takes over the regulation of ancestral gene targets. If supported, H2 would uncover the evolution of upstream regulation of network modules underlying sexual development that could occur by natural selection or developmental systems drift. This would be supported by finding a similar set of regulatory targets and functional annotations for non-orthologous TFs between species.

H3: New hub, different targets. H3 implies the overhaul of the sexual development network either in its entirety, or for some of its modules, and would be supported if major differences are found in the identity of TF hubs, their connectivity, and their target genes, which could be carrying out either the same function as the ancestral hub and targets, a new function (neofunctionalization), or no function (pseudofunctionalization).

Materials and methods

We constructed models of gene-TF interaction networks for both *Chrysemys* and *Apalone* using PANDA as implemented in the R package pandaR [33,34]. As input to construct the networks, pandaR takes gene expression data, TF binding site data, and protein-protein interaction data. PANDA utilizes a message passing algorithm to integrate and find agreement among multiple datasets, *via* similarity calculations, building a consensus network with predicted regulatory relationships [33]. We describe the generation of each of those datasets below.

Gene expression dataset

We used RNA-seq data from a previous study [19], which we generated by incubating eggs from both *Chrysemys* and *Apalone* turtles at temperatures that are either 100% male- or female-producing in *Chrysemys* (MPT: 26°C and FPT: 31°C, respectively) following our standard protocols [35]. These temperatures are within the optimal developmental range for both species. Tissue was collected from both species across five matched stages of development [sensu a common staging table [36], instead of the species-specific criteria [37,38] and included the following tissues: stage 9 – trunks, stages 12 and 15 – adrenal kidney gonad complexes (AKGs), and stages 19 and 22 – gonads. Stages 9 and

12 precede the thermosensitive sex determination period (TSP) in *Chrysemys*, stage 15 sits at the onset of the TSP, whereas stages 19 and 22 are at the mid and late TSP. This sampling at stages 9−15 accounts for potential thermal effects on sex ratios prior to the canonical thermosensitive period detected in TSD turtles [39,40], encompasses the formation of the adrenogonadal primordium, and captures contributions from the earlier mesonephros to the developing gonad [41]. We note that sexual differentiation in *Apalone* takes place at similar stages as in TSD turtles [42]. Embryos of *Chrysemys* were presumed to be developing males or females according to their incubation temperature, while *Apalone* embryos were sexed by PCR using molecular markers [43], an improved sexing technique compared to qPCR of rRNA genes [44]. Thus, *Apalone* samples correspond to a full factorial dataset with male and female embryos developing under temperatures that represent the ancestral MPT and ancestral FPT. Two biological replicates (RNA libraries) were generated for each condition (species by stage by temperature, and by sex for *Apalone*), and each library included RNA pooled from 11−15 embryos. At least 40 M clean Illumina 150 bp paired-end reads were generated per library (with a 94–97% retention rate per library). Further details of the transcriptomic datasets were previously reported [19]. Reads were trimmed with Trimmomatic (v0.36) [45] and mapped with GSNAP (v20170317) [46,47] to a reference genome for each species: *Chrysemys* GCF_000241765.3_Chrysemys_picta_bellii-3.0.3 [18] and *Apalone* BioProject: PRJNA837702 [48]. Using StringTie (v1.3.4) [49], reads were assembled into transcripts by library, merged, and their abundance was calculated. Then, transcripts and counts were consolidated into gene models with tximport (v1.10.1) [50]. Finally, counts were TMM-normalized to correct for library size and $\log_2$-transformed to correct for heteroskedasticity using EdgeR (v3.24.3) [51].

Transcription factor binding site (TFBS) motif dataset

Promoter sequences, defined as −1.5Kb and +500 bp surrounding the transcription start site, were extracted for all annotated genes from the *Chrysemys* and *Apalone* reference genomes. While DNA sequence can turnover rapidly, DNA binding domains for TFs are highly conserved in vertebrates and recognize the same binding motifs across lineages [52–54]. Given this documented conservation, we used vertebrate TF binding matrices from the open access JASPAR Core Vertebrate database (v2020) [55]. TF position weight matrices were searched against these promoter sequences, using CiiiDER (v1.10.6) [56] with the deficit parameter set to a highly stringent 0.05 to create a map indicating whether promoters contained putative binding sites for these TFs. Our approach centers the search for TFBS motifs around promoter sequences, permitting the identification of putative binding sites, as such sequences could affect gene regulation irrespective of their evolutionary origin [57–60].

Protein interaction dataset

Protein sequences and protein-protein interaction data from vertebrates were obtained from the STRING database (v11.0) [61] which included data from 41 vertebrates (30 mammals, 3 birds/reptiles, 1 amphibian, and 7 fishes). In parallel, we obtained the longest translated CDS for proteins present in the *Chrysemys* genome [18]. Because PANDA focuses on gene-TF interactions, the list of *Chrysemys* proteins was filtered down to retain TFs also present in the JASPAR core vertebrate database (v2020). Because the data on protein-protein interactions draws upon other vertebrate species, we employed stringent filtering to increase the likelihood that results would be conserved in turtles. Using a reciprocal best blast approach (blastp), we compared the sequences of the STRING interacting proteins to the subset of *Chrysemys* TFs and did a final filtering step resulting in a list of TFs with a percent identity of ≥90% and resulting query coverage of ≥99%. STRING proteins and their interactors that passed through these filters were retained and assumed to represent protein interactions likely present in *Chrysemys* due to their high level of homology. For *Apalone*, protein sequences from *Chrysemys* representing putative interacting proteins were searched (tblastn) against the *Apalone* genome [48] and their presence was confirmed, such that the same protein interaction file was used as input for both species.

Building models of gene – transcription factor interaction networks with PANDA

For *Chrysemys*, each gene expression dataset per temperature (26 and 31°C) consisted of ten gene expression libraries, encompassing two biological replicates from five developmental stages, yielding 20 libraries total. These temperature-specific libraries were used as input to predict MPT- and FPT-networks in PANDA (Cpi-Female-31°C network and Cpi-Male-26°C network). Because each incubation temperature produced both sexes in *Apalone*, there were 40 datasets for this GSD species, i.e., two replicates per stage for each sex-by-temperature combination. Sex-by-temperature sets were used as input in PANDA to generate 4 networks (Asp-Female-26°C, Asp-Female-31°C, Asp-Male-26°C, and Asp-Male-31°C). We will refer to these networks as Cpi-FPT, Cpi-MPT, Asp-F26, Asp-M26, Asp-F31, and Asp-M31 hereafter.

The PANDA algorithm was implemented with the R package pandaR (v1.22.0) [34], using as input the gene expression, TFBS motif, and protein-protein interaction datasets described above. Default settings were used in most cases, but the mode was set to 'intersection' to only include TFs present in the gene expression dataset while keeping network size to a manageable scale. Following network construction, it was discovered that the mode option works differently than described in the pandaR manual, so we manually confirmed which TFs in the final network were expressed in our transcriptomes and disregarded unexpressed TFs when interpreting the results. Networks produced by PANDA consist of gene-by-TF matrices populated with similarity scores (akin to Z scores) describing the likelihood that an edge (i.e., the connection between a gene and TF that defines a regulatory relationship) is true, where positive values represent greater support for an edge and negative values represent lesser likelihood that an edge is true.

To test for differences between networks, we used a permutation approach implemented with a custom R script to build a test distribution of networks (Fig 2). For this, we first built a gene (row) by library (column) matrix populated with gene

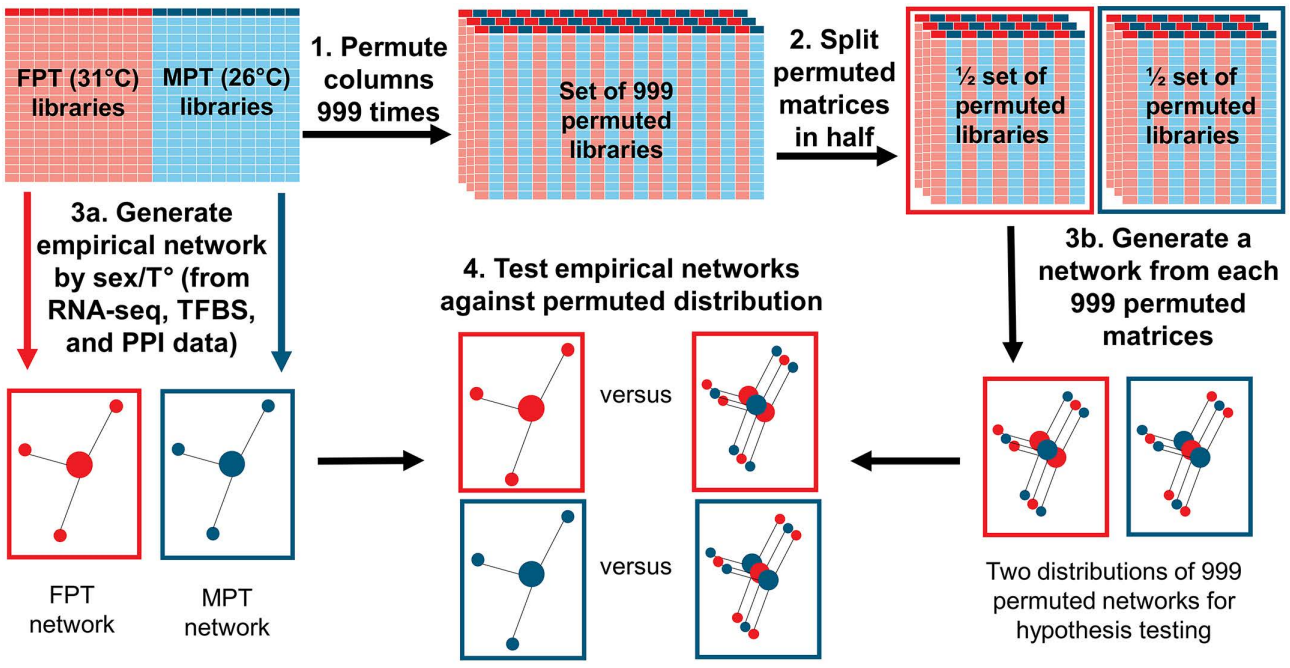


Fig 2. Pipeline of the permutation procedure used to generate random distributions for network comparisons using the *Chrysemys* data as an example. First, a matrix containing normalized gene expression values for all 20 libraries (red columns = FPT/female libraries, blue columns = MPT/male libraries) were permuted 999 times to generate 999 matrices with random column order. Second, each of these 999 matrices were split in half. Third, each 10-column set of submatrices was used as input to generate a random distribution of networks. Fourth, each empirical network derived from the original libraries was tested against one of the random distributions. The same process was used for *Apalone*'s 40 libraries for *Apalone* as detailed in the text. TFBS = Transcription Factor Binding Site; PPI = Protein-Protein Interaction.

https://doi.org/10.1371/journal.pone.0353280.g002

expression values (20 columns in the case of *Chrysemys*). Then, we ran 999 permutations randomizing the order of the libraries (columns) in the matrix. The resulting 999 permutated matrices were split in half (columns 1–10, columns 11–20 for *Chrysemys*) to generate two sets of 999 matrices with permuted columns, and a network was generated (as described above) from each set to obtain two random distributions of 'permuted' networks against which to test each empirical network. The empirical FPT network was tested against one distribution while the empirical MPT network was tested against the second distribution. Likewise, for *Apalone*, the initial 40-column matrix (for the 40 libraries) was also permuted 999 times, and these randomized matrices were split in four groups (columns 1–10, 11–20, 21–30, 31–40) to generate four sets of 999 permuted matrices. A network was generated from each set of permuted matrices in PANDA to obtain four random distributions against which to test each empirical network (Asp-F26, Asp-M26, Asp-F31, and Asp-M31).

Analysis of differential gene – transcription factor networks

We conducted within-species comparisons of gene-TF networks which tested for differences between temperatures in *Chrysemys* (Cpi-FPT vs Cpi-MPT), while for *Apalone*, comparisons tested for differences between-sex per-temperature (Asp-F26 vs Asp-M26, Asp-F31 vs Asp-M31), and between-temperatures per-sex (Asp-F26 vs Asp-F31, Asp-M26 vs Asp-M31).

Networks consist of nodes connected by edges. An edge is a vertex connecting a gene to a TF, representing the presence of an interaction. We tested for edge weights that were significantly different between two networks of interest. Using a t-test, the difference between each predicted edge (e.g., network *i* edge minus network *ii* edge) was compared to the average difference for that edge between all permuted pairs of networks. Significance was assessed following a Benjamini-Hochberg correction for multiple comparisons.

In addition to examining differential network edges, we also examined differences in network targeting patterns, of which there are two types [62,63]: gene in-degree and TF out-degree. Gene in-degree describes how many edges in the network point to a gene, while TF out-degree, describes how many edges point from a TF to various genes. Thus, these values help identify which genes and TFs of the networks are highly connected, and whether differences in the in-degree and out-degree patterns exist. In-degree and out-degree values were calculated with the pandaR function calcDegree() which sums edge weights for a particular vector (i.e., the row of TFs targeting one gene, or the columns of genes targeted by one TF). Similarly, for the differential edge calculation, a t-test was performed to assess differences in targeting patterns between pairs of empirical networks relative to the test distribution of differences in targeting patterns for all pairs of networks. Significance was assessed following a Benjamini-Hochberg correction for multiple comparisons.

We also assessed overall differences in the gene:TF networks by calculating the sum of squares of each network's matrix and comparing the difference of the sum of squares between empirical networks to the distribution generated by calculating the differences in the sums of squares of all pairs of permuted networks. Thus, we assessed networks for differences at the edge (individual gene-by-TF targeting patterns), vector (TF regulatory patterns for collective gene targets), and matrix (whole network regulatory patterns) levels.

Principal components analysis and trajectory analysis

We carried out a modified trajectory analysis [64] to test for differences in the regulatory targeting patterns of orthologous TFs. For this, we first filtered all six networks (2 from *Chrysemys* and 4 from *Apalone*) to identify the set of genes and TFs shared between species and transformed negative edge-weights to zero to denote a lack of relationship. Principal components analysis was then performed on the edge weights representing the genes targeted by each TF. The resulting principal components plot where the differences in targeting patterns of TF hubs are visualized constitutes the "regulome space". These networks were further filtered to only include TFs with an average expression level of >1.5 $\log_2$ (TPM) across all libraries in the initial input gene expression data (to rule out negligibly expressed TFs) and that were present in all 6 networks. Next, the principal components were subjected to the modified trajectory

analysis [64], which connects centroids of orthologous TFs by a vector in regulome space. The centroid is the position of a TF in the regulome space informed by the genes it regulates in the networks within each species (and is calculated from each set of species-specific networks), and the distance between centroids measures how similar or different TFs are relative to one another in the genes they are predicted to regulate between species. Longer vectors denote greater divergence in the gene targets of ortholog TFs between species, compared to TFs connected by shorter vectors in the PC Euclidian plane. To measure these distances between species for each TF, we modeled gene targets as a function of TF, species, and their interaction (linear model: Gene Targets ~ TF + Species + TF: Species). Distances between the centroids of the principal components of the target genes for a particular TF per species were calculated. We then generated a distribution of distances under the null hypothesis that there were no differences between species (no effect of species on TF). This corresponds to the prediction that no evolution has occurred in the regulatory role of these orthologous TFs since *Chrysemys* and *Apalone* split ~175 mya (timetree.org) (hypothesis H0). We tested the distances of each TF between species against this distribution using a permutation test and applied a Benjamini-Hochberg correction for multiple comparisons with an exploratory FDR of 0.1 given our sampling limitations. Using this level of FDR the top ~ 5% of distances of TFs and those belonging to the right-most distribution in our bimodal distribution of distances were considered significant. Non-significant distances between orthologous TFs between species reject hypothesis H1 and may denote TF hubs conserved between lineages in their target patterns (supporting hypothesis H0), whereas orthologous TF hubs with significantly longer distances would have diverged between species in the identity of the genes they regulate (hypothesis H1) (Fig 1). We tested hypothesis H2 by measuring trajectory distances of non-orthologous pairs of TFs between species. Here, we identified interspecific trajectories that were shorter than expected under the null hypothesis, indicating non-orthologous (analogous) TFs that converged on the same gene targeting pattern between species (supporting hypothesis H2). Additionally, we confirmed that these trajectories were shorter than the distance to their respective orthologous TFs (albeit not significantly shorter since they were all above the critical value of the 5% quantile). Hypothesis H3 was tested by consilience with the other hypotheses.

Gene ontology overrepresentation analysis of networks

The PANTHER (v17.0 – date: 2022-02-02) online GUI [65] was used to conduct overrepresentation analysis of gene targets of TFs of interest. We used a Fisher's Exact Test with an FDR correction to determine which gene ontology (GO SLIM) terms (molecular function, cellular component, and biological process) were overrepresented in the targets [66], as well as if any PANTHER pathways [67] or PANTHER protein classes were overrepresented. Since our focal species are non-model organisms that are not represented in the PANTHER databases, we first mapped the translated CDSs from *Chrysemys* to PANTHER IDs using PANTHER HMM scoring tools (pantherScore2.2) to score our sequences against the PANTHER HMM library (v17.0), following the instructions provided by the PANTHER developers. In the case of duplicate hits due to redundancy in the *Chrysemys* genome, we prioritized the result to those with the highest bitscore. Since *Apalone* annotations were based on the *Chrysemys* genome, we used the mappings obtained from *Chrysemys* CDS sequences to transfer the corresponding annotations to genes in the *Apalone* networks. Only TFs with at least 50 known gene targets prior to uploading to PANTHER were included in the overrepresentation analysis, as functional annotation results can be sensitive to input list size [68,69]. Additionally, to focus the analysis on gene targets with the highest support in the network models, gene targets were filtered to retain those with an edge weight in the top 5% of all edge weights. Our approach resulted in sets exceeding the 50-gene benchmark, as most sets analyzed had 100s or 1000s gene targets in their input list. Tabular results of the analysis were downloaded and saved locally. The background gene set included all genes present in the network, but because not all genes mapped to panther IDs the total effective number was smaller (CPI: 16489 genes, ASP: 11386 genes).

Transcription factor functional similarity analysis via calculation of semantic similarity

The resulting sets of overrepresented terms of TF gene targets were compared for semantic similarity with GOGO [70] to determine their degree of functional similarity. Shifts in functional annotation are suggestive of putative changes in function that require functional validation (referred to as changes in function hereafter for simplicity). GOGO is a hybrid algorithm for semantic similarity calculations that uses both the topology of the directed acyclic graphs (DAG) that make up the ontology (which informs ancestor-child term relationships) and considers the number of children nodes of a term (which reveals the information contained in a term). Thus, it allows us to impartially assess how similar two lists of gene ontology terms are to one another which can be hindered by their hierarchical nature. We updated the DAGs used by the program to match the same reference ontologies used to run the overrepresentation tests (PANTHER v17.0). We used the gene_list_comb.pl script to calculate semantic similarity of the sets of statistically significant GO terms returned for the gene targets of a TF in a particular network. We then compared the similarity scores, which range from zero (no similarity) to one (perfect overlap), to assess the degree of putative functional similarity of TF targets for orthologous TFs across networks. We used a Mann-Whitney U test to evaluate whether there were significant differences in semantic similarity for the set of within-species comparisons (all *Chrysemys* by *Chrysemys* and all *Apalone* by *Apalone* contrasts) relative to the set of between-species comparisons (all *Chrysemys* by *Apalone* contrasts) and applied a Bonferroni correction for multiple comparisons.

Subnetworks

Because the final networks obtained from PANDA for *Chrysemys* contained 2,883,632 edges, we also generated subnetworks to focus our attention on the most strongly supported edges, by filtering networks for the edges with an arbitrary selected Z score > 10 (which corresponds to the top 0.03% of edges for *Chrysemys* and *Apalone*). Subnetworks were visualized in Cytoscape (v3.9.0) [71], and the hubs and their targets were identified using the function targetedGenes() for overrepresentation analysis of gene ontology functional terms.

All scripts used for the analyses are included in the Supporting Information.

Results

Putative core network components of turtle sexual development

Models of gene-TF interaction networks were constructed using PANDA [33,34] with matched-stage RNA-seq data from a previous study of *Chrysemys* and *Apalone* embryos [19] (trunks at stage 9, adrenal kidney gonad complexes at stages 12 and 15, and gonads at stages 19 and 22), transcription factor binding sites from their reference genomes [18,48], and vertebrate protein-protein interaction data [61], which yielded two networks for *Chrysemys* (Cpi-Female-31°C and Cpi-Male-26°C), and four networks for *Apalone* (Asp-Female-26°C, Asp-Female-31°C, Asp-Male-26°C, and Asp-Male-31°C). We will refer to these networks as Cpi-FPT, Cpi-MPT, Asp-F26, Asp-M26, Asp-F31, and Asp-M31 hereafter. For *Chrysemys* and *Apalone*, all network pairs within species were nearly identical when analyzed for differential edges (an edge is a network vertex connecting a gene to a TF, representing the presence of an interaction), differential targeting patterns (i.e., gene in-degree and TF out-degree patterns, which describe how many edges point to a gene, and how many edges point from a TF to various genes, respectively), and overall network differences at the full matrix level (i.e., *Chrysemys*: Cpi-MPT vs Cpi-FPT; *Apalone*: Asp-M26 vs Asp-F26, Asp-M31 vs Asp-F31, Asp-M26 vs Asp-M31, and Asp-F26 vs Asp-F31). Namely, no differential edges or differences in targeting patterns were detected after Benjamini-Hochberg correction, and the sum of squares calculation assessing overall network differences was also non-significant ($p > 0.2$ in all cases, Table 1). The same was true if networks were built based on only differentially expressed genes. This overall similarity among networks at the global level is likely due to the small size of the dataset and the pooling of gene expression data from five developmental stages. This caveat implies that the results described here are conservative, as they represent

Table 1. Sum of squares result from the overall network comparison.

Network Comparison	Sum of Squares	Pvalue
Chrysemys 26°C vs 31°C	330214.43	0.677
Apalone Female 26°C vs Male 26°C	226941.63	0.376
Apalone Female 31°C vs Male 31°C	264538.08	0.224
Apalone Female 26°C vs Female 31°C	146894.62	0.853
Apalone Male 26°C vs Male 31°C	237478.87	0.329

https://doi.org/10.1371/journal.pone.0353280.t001

the strongest signals that stand out despite our sampling limitation. The coarse global comparison approach identified potentially evolutionarily conserved developmental signals common to all conditions and embryonic stages (not only within but also between species as described below) that may represent presumptive core components of turtle developmental processes to be functionally validated in future studies or ruled out if larger sampling uncovers differences that passed undetected here. On the other hand, the subtle sex- or temperature-specific differences that were too weak to be detected with this initial global method (masked by the broad overall similarities), were revealed by quantitative hypothesis testing. This included 89 out of 148 turtle TFs from the full networks that were expressed in the time-course transcriptomes of both *Chrysemys* and *Apalone* and thus permitted further evolutionary analyses between species.

Principal components and trajectory analysis

We employed principal components (PC) analysis on the edge weights representing the genes targeted by each TF to more clearly discern the patterns present in these hyperdimensional 'omics data, after retaining only genes and TFs shared between species across all six networks, transforming negative edge-weights to zero to denote a lack of relationship, and excluding negligibly expressed TFs with average expression <1.5 $\log_2$(TPM) [TPM = transcripts per million]. Next, the principal components were subjected to a modified multivariate trajectory analysis [64] to test for differences in the regulatory targeting patterns of orthologous TFs. We compared the length of the vector that connects centroids of orthologous TFs in regulome space to the length predicted under the null hypothesis (H0) that there were no differences between species (Fig 3A-C). Regulome space provides a measure of how similar or different TFs are relative to one another in the genes they are predicted to regulate between species. PC1 and PC2 captured 25.2 and 5.1% of the variation, respectively (Fig 3D), while 888 PCs explained all the variance, reflecting the high complexity of these networks and the many factors that contribute to their variation.

Results from the multivariate trajectory analysis on this principal components' space (the regulome space) revealed 50 of 89 TFs that supported the null hypothesis H0 (same hub, same targets) as they were conserved in their regulatory targets (Fig 3A). Hypothesis H1 (same hub, different targets) (Fig 3B) was supported by the remaining 39 TFs that significantly diverged from their ortholog in the identity of genes targeted or in the strength of their connection (Fig 3D). Next, we conducted overrepresentation tests of the functional annotations of the predicted regulatory targets of these 39 TFs obtained using The Gene Ontology and calculated the similarity between orthologs using semantic similarity (see methods for details). We found 5 TFs (ARID3B, EMX2, LHX9, LIN54, and MEOX2) exhibited significant overrepresentation test results across all 6 networks (FDR of 0.05), enabling full cross-species comparison of their semantic similarity for hypotheses testing of the three alternative explanations of their divergence in regulome space (Table 2). Semantic similarity considers the gene ontology terms and graph structure to assess differences in functional annotation (i.e., putative functional role) [70]. We analyzed these 5 TFs to determine whether the functional role of their new targets remained conserved despite the turnover in target identity (hypothesis: H1A), whether a new functional role was acquired (hypothesis H1B), or whether a clear function was lost (hypothesis H1C) (Fig 1), and found ARID3B supported H1A, while EMX2, LHX9, LIN54, and MEOX2 supported H1B. Potential support for hypothesis H2 that a non-orthologous TF took over the regulation of an ancestral TF hub, was found for

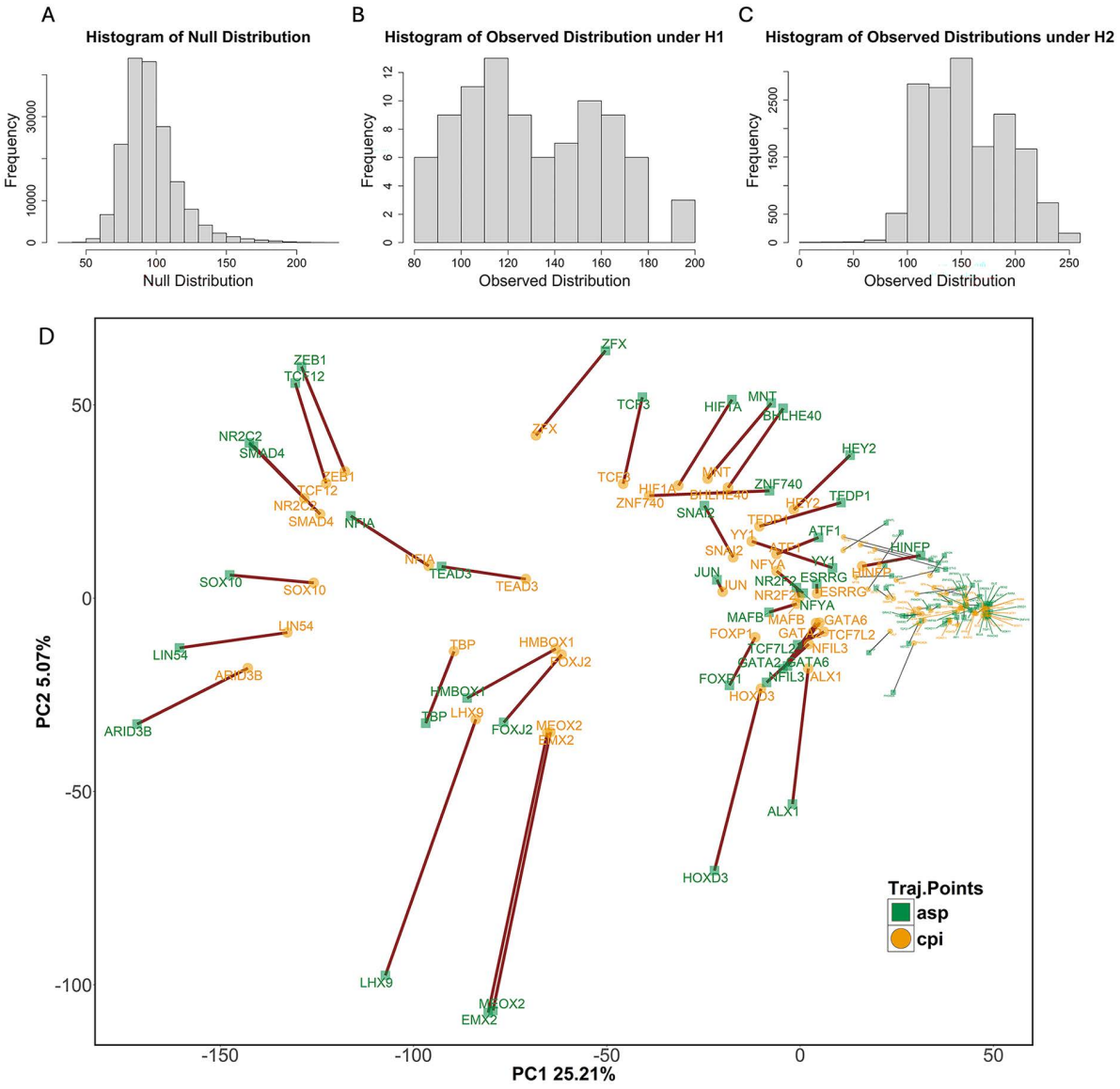


Fig 3. Trajectory analysis of the evolution of 89 transcription factors between *Chrysemys* and *Apalone*. Null (A) and observed (B and C) empirical distributions of distances (trajectory magnitudes) between orthologous TFs (B) and non-orthologous TFs (C) in regulome space (D). Trajectory magnitudes are based on the edge weights between TFs and their gene targets which are represented as effect sizes (Z scores). The distribution in panel B was used to test hypothesis H1, i.e., whether trajectories between orthologous TFs were longer than expected under the null hypothesis H0 (that no evolution occurred between these two turtle lineages over 175 my). The distribution in panel C was used to test hypothesis H2, i.e., whether trajectories between non-orthologous TFs were shorter than expected under the null hypothesis H0, which would indicate that non-orthologous TFs converged between species on a common set of gene targets. (D) Greater divergence between species in the gene targeting patterns of orthologous TFs is denoted by longer vectors (greater Euclidean distance in the principal components regulome space) between *Apalone* and *Chrysemys*. Thicker brown lines indicate significantly longer trajectories than expected, whereas thinner gray lines indicate trajectories of length expected by chance (supporting H0).

https://doi.org/10.1371/journal.pone.0353280.g003

a single TF in the GSD *Apalone* (ZBED1) that is closer in regulome space than expected under the null H0 to 12 TFs in the TSD *Chrysemys* (BACH2, BCL6, CTCF, GLI2, GLIS3, IRF1, MTF1, NR2F6, PKNOX2, RXRA, TGIF1, ZNF410). Intriguingly, the ZBED1 ortholog was not significantly farther apart than expected (failed to reject H0), thus, ortholog targeting patterns

Table 2. Semantic similarity in biological process (BP), cellular component (CC) and molecular function (MF) for transcription factors that evolved significant differences in targeting patterns between *Chrysemys* and *Apalone* as determined by trajectory analysis of the principal components regulome space.

Transcription Factor	Trajectory Analysis *P* value	Semantic Similarity Differences Between Species *P* value	Between Species Gene Overlap	Within CPI Gene Overlap	Within ASP Gene Overlap
ARID3B	0.072	BP, CC, and MF: all NS	9.3-11.6%	44.7%	53.7-67.3%
EMX2	0.054	**BP: 0.022**	3.9-5.7%	51.3%	36.4-52.8%
LHX9	0.087	BP: NS; **CC: 0.014**	4.9-6.8%	49.0%	39.6-53.5%
LIN54	0.072	**BP: 0.037; CC: 0.025**	5.7-7.5%	39.5%	41.8-53.5%
MEOX2	0.042	**BP: 0.015;** CC: NS	3.6-5.7%	50.5%	34.9-52.2%

Semantic similarity indicates how similar the sets of gene ontology terms annotated to a TF were when compared between species while accounting for hierarchical graph structure. P-values are provided for TFs with significant differences in their semantic similarity between species at an exploratory $\alpha = 0.1$ which corresponded to the top 5% of TFs that occupied the upper mode of the observed distribution (Fig 3B). The degree of overlap in the sets of genes regulated by each TF is also provided, including: the range of gene overlap for all *Chrysemys* vs all *Apalone* (Between Species), *Chrysemys* MPT vs *Chrysemys* FPT (Within CPI), and the range of gene overlap for all *Apalone* vs all *Apalone* (Within ASP) to illustrate the degree of change in gene targeting patterns between species. See the Supporting Information for the full list of overrepresentation results. NS = Non-significant.

https://doi.org/10.1371/journal.pone.0353280.t002

did not differ between species. Combined, these results suggests that either *Apalone* ZBED1 acquired a new regulatory role without giving up its ancestral regulatory role, or alternatively, that the 12 TFs in *Chrysemys* slightly converged on ZEBD1's targets. Lastly, while the biologically-relevant analysis includes the 4 networks from *Apalone* because both sexes developed at each incubation temperature in this GSD species, we carried out a sensitivity test by rerunning the trajectory analysis using both *Chrysemys* networks and pairs of male and female *Apalone* networks as listed in Table 1, and found that results are qualitatively robust (the same 39 TFs remained ranked in the top 39 positions, and the top 37 retained significant unadjusted p-values). We thus restrict the follow up discussion to these 37 TFs.

New targets of ARID3B, a gene linked to primary cilia sensory mechanism, carry out a conserved function in support of hypothesis H1A

ARID3B, a factor expressed in the Leydig cells of human and mouse testis [72] that affects the expression of *Wnt1* and other genes in the placenta [73], was highly and constitutively expressed throughout development in both turtle species and both sexes [19]. Here, ARID3B was more distant in regulome space between species than expected under the null hypothesis (H0), and relatively low overlap was detected in the identity of ARID3B's gene targets between species (Table 2). Yet, no significant differences in semantic similarity were detected when contrasting between versus within species comparisons, indicating a conservation of ARID3B's function despite a change in gene targets (hypothesis H1A). This observation supports the notion that developmental systems drift affected the evolution of ARID3B's gene targeting pattern between species.

When examining individual contrasts, semantic similarity of ARID3B targets was much lower between sexes in *Chrysemys* relative to within-*Apalone* contrasts, particularly for molecular function. Specifically, ARID3B targets at Cpi-FPT related to channel activity and membrane transport, which could implicate ARID3B in the epigenetic regulation of TSD female development [21,22], but mostly to cytoskeletal protein binding (tightly linked to primary cilia formation and maintenance) at Cpi-MPT. Notably, ARID3B terms relate directly to primary cilia for males incubated at 26°C in both species.

EMX2, LHX9, LIN54, and MEOX2 are linked to primary cilia and support hypothesis H1B (same hub directs new function with different targets)

These TFs differed significantly more between *Chrysemys* and *Apalone* in their targeting patterns than expected under the null hypothesis H0 (Table 2), reflecting an evolutionary change in their regulatory subnetworks. Furthermore, they

showed significant differences in functional annotation when testing for semantic similarity. EMX2 and MEOX2 showed a significant difference in semantic similarity for the biological process ontology, LHX9 for the cellular component ontology, LIN54 for both, and all showed changes in function that accompanied the change in gene targets between species (Table 2), supporting hypothesis H1B (retention of the TF hub while gene targets changed in identity and function). Notably, all four TFs returned overrepresentation terms for primary cilia. LIN54 is also related to Wnt signaling which primary cilia help sense [74]. Additionally, all four TFs diverge somewhat among sex/temperature within-species networks (Table 2), revealing a lability between sexes or species that renders them candidates of interest underlying the transition of sex determination.

EMX2 exhibited the lowest semantic similarity between the Asp-M31 network (an ancestrally feminizing temperature) and all other *Apalone* networks. EMX2 is essential for gonadal and urogenital development in eutherian mammals [75] and a marker of the bipotential gonad early in embryogenesis [76], a time when Wnt signaling also participates [77]. This result is consistent with previous genome-wide developmental-transcriptomic trajectory analysis showing that the most sexually dimorphic gene expression in this GSD turtle occurs at the ancestrally feminizing 31°C temperature. In *Apalone, Emx2* was upregulated in females at stages 19 and 22 and downregulated in males at 31°C [19], whereas in *Chrysemys, Emx2* showed monomorphic expression [19,78]. The opposite was not true. Namely, the ancestral masculinizing temperatures (26°C) did not induce greater divergence of the Asp-F26 network as no reduced semantic similarity was detected when comparing to all other *Apalone* networks. Consistent observations were made during the between-species comparisons. That is, Asp-M31 networks returned fewer terms than all other networks, which overlapped largely with other *Apalone* networks, but not at all with *Chrysemys*, and thus showed the lowest semantic similarity with *Chrysemys* networks. Terms in Asp-M31 were related to cell projection and microtubules – possibly pointing to general primary cilia related-terms (and explicit primary cilia terms were present in all other *Apalone* networks). Meanwhile, both *Chrysemys* networks returned terms related to anatomy and multicellular development with Cpi-FPT's terms related to the nervous system and Cpi-MPT's terms related to transcription and the immune system (functions linked to primary cilia in other species as detailed in the discussion).

For **LHX9**, another bipotential gonad marker [76,77] important for gonadal development in turtles and mammals [79–82], the functional ontology terms of gene targets for *Apalone* were associated mostly with the cytoskeleton, which is important for various cellular structures and processes including a key role for the formation of primary cilia [83,84]. For *Chrysemys*, terms were associated with ion channels many of which reside in the ciliary membrane among multiple cellular locations. This supports LHX9's mechanistically important role to relay temperature cues in TSD animals [20,85], and suggests the evolution of GSD in *Apalone*'s lineage may have released LHX9 from its TSD function. Consistent with this observation, the within-species cellular component semantic similarity for LHX9 was generally quite high for *Apalone* but more moderate for *Chrysemys*. This suggests the hypothesis that LHX9 is perhaps more plastic in TSD *Chrysemys* and more canalized in GSD *Apalone*. Consistently, *Lhx9* in *Chrysemys* is upregulated at MPT (26°C) throughout the thermosensitive period (stages 15, 19 and 22) whereas in *Apalone, Lhx9* retains this ancestral upregulation at 26°C throughout stages 15, 19, and 22, but it is also upregulated in stage 19 females compared to males irrespective of temperature, and in stage 22 females at 31°C [19], suggesting a putative evolutionary shift in expression and functional regulation with respect to sex, but not temperature.

LIN54, a factor involved in development and reproduction in the genus *Drosophila*, *Caenorhabditis elegans* [86,87], and perhaps mammals [86,88], is a core subunit of the DREAM/LINC complex that regulates DNA repair and the cell cycle [86,88–91]. The primary cilium is linked to the cell cycle as the centrosome that comprises the basal body of the primary cilium becomes the mitotic spindle of dividing cells [32,83]. LIN54 showed significant differences in semantic similarity for both biological process and cellular component between species despite showing stable expression throughout development in both sexes in *Chrysemys* and *Apalone* [19]. In *Apalone* these differences were largely driven by Asp-M26 which returned terms related to primary cilia, while other *Apalone* networks returned fewer or more general biological process terms, and

cellular component terms related to the nucleus. In contrast, *Chrysemys* terms were generally related to the nervous system and to neuron and ion/cation channel and cellular periphery at Cpi-FPT, but to the immune system, Golgi-vesicle transport, muscle cell-related, cytoskeleton/microtubule, nucleolus, and ribosome terms at Cpi-MPT. Importantly, previous studies have shown that many of these components have ties to primary cilia directly or indirectly [[32] and references therein].

MEOX2 is better known for its involvement in mesoderm differentiation [92,93] and limb development [94] but is also tied to nociception of inflammatory stimuli [95] in vertebrates. The biological process terms retrieved here for MEOX2 were strongly indicative of primary cilia and related components for *Apalone*, while *Chrysemys* networks were characterized by terms related to development for both networks with nervous system terms returned for Cpi-FPT and immune system for Cpi-MPT. Although differences in the semantic similarity of cellular component were not significant for within versus between species comparisons, the semantic similarity value between male and female *Chrysemys* was very low (0.172), unlike in *Apalone* (> 0.5 for all contrasts). This was due to the overrepresentation of calcium channel terms in Cpi-MPT but not Cpi-FPT networks, another important cellular component for relaying environmental cues during TSD gonadal development [21,22], and consistent with recent work connecting calcium to male development via aldosterone production in *Trachemys scripta* [96] (*Trachemys* hereafter).

Targeted comparison of networks: subnetwork analysis also points to primary cilia

We also queried the networks qualitatively for subtler but potentially biologically important similarities and differences, focusing on hubs from highly supported subnetworks (those with edge scores $Z > 10$) and comparing (a) the identity of the TF hubs themselves, (b) the similarity in the identity of their gene targets, and (c) the functional annotations and overrepresentation of their gene targets. We identified 26 TFs of interest (Table 3) to further examine the molecular circuitry (network topology) of urogonadal development in *Chrysemys* and *Apalone*.

The topology of these 26 TFs and their gene target interactions in the *Chrysemys* male and female subnetworks obtained from PANDA were nearly identical to each other in their pattern of gene targeting (Table 3), and the same was true within *Apalone* subnetworks. Thus, we focused on interspecific patterns. Between species, the same set of TF hubs were highly supported in both species, yet their highest supported gene targets differed considerably between *Chrysemys* and *Apalone*. Some TF hubs in the subnetwork were lowly expressed in only one species, maybe because they experienced a loss in activity (KLF13, RXRG, SPI1 in *Chrysemys*; GRHL1 in *Apalone*). They are returned as a hub likely because TF binding sites (and thus their regulatory potential) still exist in the promoter region of ancestral gene targets, possibly because they are still active in another context (e.g., pleiotropy).

Of these 26, six subnetwork hub TFs exhibited overrepresented biological functions exclusively in *Chrysemys* (CTCF, RFX2, RFX4, TCF3, ZEB1, and ZNF143) and virtually identical annotation terms at Cpi-MPT and Cpi-FPT for each TF, suggesting their likely role in general non-dimorphic sexual development. But importantly, gene targets for each of these six TFs differed greatly between species (0.68–11.5% overlap). This low overlap between species may be due to the less complete annotation of the *Apalone* genome compared to the *Chrysemys* genome, or alternatively, it may suggest (1) a functional loss for sexual development for these TFs in *Apalone* (hypothesis H1C, pseudofunctionalization), perhaps by genetic drift and consistent with an absence of significant overrepresentation results in this GSD turtle, or (2) a change in TF regulatory roles in *Apalone* compared to *Chrysemys*, perhaps if the divergence in gene targets led to subfunctionalization (a change in regulation of a particular functional process by distributing the ancestral role across different TFs). Of note, three of these six TFs (TCF3, RFX4, and ZEB1) returned terms related to primary cilia. Moreover, RFX4 along with RFX2 play an important role in ciliogenesis, which is broadly conserved across vertebrates, and are testis regulators with RFX2 having a key role in spermatogenesis affecting ciliary and cytoskeleton remodeling genes [102,103,110–112].

Additionally, the terms related to primary cilia were overrepresented repeatedly irrespective of regulatory differences between species. Nineteen TFs returned significant overrepresentation results related to primary cilia (ARID3B, EMX2, LHX9, LIN54, and MEOX2 mentioned above, plus DLX2, HIC2, HMBOX1, HOXD3, LHX2, MSX1, NFIA, RFX4, SHOX,

Table 3. Highly supported subnetwork TF hubs identified in *Chrysemys* (CPI) or *Apalone* (ASP) using an edge weight cutoff of Z > 10 (listed alphabetically).

CPI Sub-network	ASP Sub-network	Gene Name	Overrepresentation functional annotation	Trajectory results between species (H1 test)	Hypothesis supported	Reported link to primary cilia in literature
BACH2	BACH2	BTB Domain and CNC Homolog 2	NS	NS	H2	No
BCL6	BCL6	BCL6 Transcription Repressor	NS	NS	H2	No
CREB3L1	CREB3L1	CAMP Responsive Element Binding Protein 3 Like 1	NS	NS	H0	No
CTCF	*Z < 10*	CCCTC-Binding Factor	*CPI – no for primary cilia*	NS	H2	Yes [97]
GLI2	GLI2	GLI Family Zinc Finger 2	NS	NS	H2	Yes [98,99]
Z < 10	GLIS3	GLIS Family Zinc Finger 3	NS	NS	H2	Yes [100,101]
GRHL1	*GRHL1*	Grainyhead Like Transcription Factor 1	NS	NS	H0	No
KLF13	KLF13	KLF Transcription Factor 13	NS	Absent	*Not tested*	No
MTF1	MTF1	Metal Regulatory Transcription Factor 1	NS	NS	H2	No
MYBL1	MYBL1	MYB Proto-Oncogene Like 1	NS	NS	H0	No
NR2F6	NR2F6	Nuclear Receptor Subfamily 2 Group F Member 6	NS	NS	H2	No
PKNOX2	PKNOX2	PBX/Knotted 1 Homeobox 2	NS	NS	H2	No
PLAG1	PLAG1	PLAG1 Zinc Finger	NS	NS	H0	No
RFX2	**RFX2**	Regulatory Factor X2	*CPI – no for primary cilia*	NS	H0	Yes [102]
Z < 10	**RFX4**	Regulatory Factor X4	*CPI – yes for primary cilia*	Absent		Yes [103]
RXRA	RXRA	Retinoid X Receptor Alpha	NS	NS	H2	No
RXRG	RXRG	Retinoid X Receptor Gamma	NS	Absent	*Not tested*	No
SIX2	SIX2	SIX Homeobox 2	NS	Absent	*Not tested*	No
SOX11	SOX11	SRY-Box Transcription Factor 11	NS	NS	H0	Yes [104]
SPI1	SPI1	Spi-1 Proto-Oncogene	NS	Absent	*Not tested*	No
TCF3	*Z < 10*	Transcription Factor 3	*CPI – yes for primary cilia*	Sig.	H1	Yes [105]
TGIF1	TGIF1	TGFB Induced Factor Homeobox 1	NS	NS	H2	Yes [106]
ZEB1	*Z < 10*	Zinc Finger E-Box Binding Homeobox 1	*CPI – yes for primary cilia*	Sig.	H1	Yes [107–109]
ZIC1	ZIC1	Zic Family Member 1	NS	Absent	*Not tested*	No
ZNF143	**ZNF143**	Zinc Finger Protein 143	*CPI – no for primary cilia*	NS	H0	No
ZNF410	ZNF410	Zinc Finger Protein 410	NS	NS	H2	No

TFs that did not surpass the edge weight cutoff of Z > 10 in one species are denoted as *Z < 10*. *Italic font* denotes genes with low expression in one species [defined as $\log_2$(counts) < 1 for more than half of the libraries]. **Bold font** denotes hubs whose gene targets returned significant functional annotations in a species (detailed in the Supporting Information). Significant trajectory results indicate the gene targeting patterns diverged significantly between ortholog TFs. NS = nonsignificant; S = significant; Absent = excluded from trajectory analysis due to low expression; H0 = fail to reject hypothesis H0; H1 = evidence supports H1; H2 = evidence supports H2.

https://doi.org/10.1371/journal.pone.0353280.t003

SHOX2, SMAD4, SOX10, TCF3, and ZEB1), of which six have documented ties to gonadal development, i.e., EMX2 and LHX9 (described earlier), plus LHX2, MSX1, SMAD4, and SOX10 [75,80,113–122]. Of note, these terms tended to be present in Cpi-MPT and Asp-M26 networks, suggesting a bias towards male development tied to cooler temperatures.

Shifts in regulation of known sexual development genes of interest

Taking a qualitative candidate gene approach, we also queried which TFs targeted several well-known gene regulators of sexual development: *Aromatase*, *Dhh, Dmrt1*, *Nr0b1 (Dax1)*, *Nr5a1 (Sf1)*, *Sox9*, and *Wt1*. The TFs among these genes of interest lacked position weight matrices in the JASPAR 2020 database used to obtain TF binding sites data but have been studied repeatedly in *Chrysemys* and *Apalone* [19,24,25,78,123–126]. We focused on expressed TFs targeting these genes of interest and identified those whose average edge weight difference between species-specific networks was greater than 3 (a difference of 3 between networks was chosen as qualitatively indicative of substantial differences because the top 5% of edges in these networks corresponded to values greater than 3). Using this metric, TBX20 emerged as a candidate regulator of interest for *Aromatase* in *Chrysemys*, and HNF4A, IRF1, and PAX3 as regulators of interest of *Sox9* in *Apalone*, while NFIA and CTCF are putative regulators of interest for *Dhh* in *Chrysemys*. CTCF is a gene affecting 3D chromatin structure which differs between turtles and other amniotes [48] and is linked to male germline development [127,128]. TFs that showed a greater targeting pattern of *Dhh* in *Apalone* relative to *Chrysemys* were ARID3B, EMX2, LHX9, and MEOX2, identified by our trajectory analysis described earlier, plus ALX1, BARHL2, BHLHE40, ELF5, HESX1, HEY2, HIF1A, ISL2, LHX2, LHX8, MSX1, MNT, and VAX1. Many of these TFs have previously been linked to sexual development and reproduction, with some related to gonadal establishment and development [EMX2 [75,113]; LHX2 [115,116]; LHX9 [80]]; ELF5 to epididymis [129–131]; HIF1A to steroidogenesis in granulosa cells in the ovary [132]; and others to germ cell development [BARHL2 to undifferentiated spermatogonia [133,134]; LHX8 to oocyte development [135,136]; MSX1 to meiosis and germ cell migration [118,120]].

Discussion

Extensive fragmentary data suggest that the molecular architecture of vertebrate sexual development has evolved among disparate lineages at both the upstream regulators of sex determination and at the downstream mediators of sex differentiation, recycling some genes again and again [1,4,137]. To our knowledge, our study is the first to build and compare species-specific gene-transcription factor regulatory networks of urogonadal development between two vertebrates in the same Order that possess contrasting sex-determining mechanisms, to uncover putative key steps during the evolution of sex determination in these two lineages, by testing for conservation or divergence of modular components built using data from matched time-course sampling. TF hubs identified in *Chrysemys*, a turtle that has retained the TSD condition that is ancestral to turtles were compared to their orthologs in *Apalone*, a turtle with an evolutionarily derived ZZ/ZW GSD mechanism [30,31,138], to assess the similarity of the identity and functional annotations of their gene targets. While *Chrysemys* has been used as proxy for the ancestral TSD condition in turtles in evolutionary analyses [138], we note that these turtle lineages continued evolving since their split ~175 Mya (timetree.org), such that differences between species may not be attributable solely to changes in the softshell turtle family to which *Apalone* belongs. Indeed, further research with additional taxa is warranted to fully test the directionality of the evolutionary changes inferred here.

In general, gene regulatory networks evolve by altering hubs, their targets, or the strength of their connections, and we found evidence consistent with the notion that all these processes may have been at play during the evolution of turtle sex determination. Our results from the analysis of 89 TF hubs sufficiently expressed in the transcriptomes of *Chrysemys* and *Apalone* [19] to enable testing, countered the hypothesis that the evolution of GSD required a complete overhaul of the regulatory network of sexual development (ruling out hypothesis H3, Fig 1). Instead, our findings indicated that first, most of these TFs (50 out of 89) support the null hypothesis H0 that some TFs hubs and their targets are conserved between species, perhaps representing core components of the regulatory network of turtle sexual development. Alternatively,

perhaps subtle but biologically important differences in these modules passed undetected that would be revealed with more extensive sampling in the future. Second, 37 other TFs did diverge in the downstream genes they target, supporting hypothesis H1. The inspection of their putative function (assessed by their functional annotation) indicated that some of these 37 TFs retained their ancestral function (hypothesis H1A), and some gained a new function (hypothesis H1B) (discussed below). The remaining two TFs were excluded after the sensitivity test. Interpretation of H1C that TF targets lost their ancestral function is challenging as absence of evidence does not necessarily equate to evidence of absence, because lack of annotations might reflect incomplete datasets instead. Indeed, we did observe that 14 of the 37 TFs returned significant functional annotations for one species but not for the other (considering all 5 ontologies tested against, which include molecular function, cellular component, biological process, PANTHER protein class, and PANTHER pathways). Among these, there was a strong bias (13/14 cases) towards absence of functional annotations in *Apalone*, so we interpret this result cautiously, as it could be caused by the lower annotation of the *Apalone* genome compared to *Chrysemys*. Otherwise, this result would suggest an extensive pseudofunctionalization of the molecular circuitry underlying sexual development in this GSD turtle that requires further functional validation. The one case which solely returned functional annotations for *Apalone* was ESRRG, a steroid receptor, although most terms returned were general or related to RNA metabolism or gene expression. We found a single putative case of a TF (ZBED1) in the GSD *Apalone* that either took over the control of conserved targets (hypothesis H2) while retaining its ancestral function, or alternatively, of 12 TFs in *Chrysemys* that converged on ZEBD1's targets. Overall, our findings agree with the conservation of higher order regulatory network architecture documented in eukaryotes, and that substantial divergence has accrued in the identity and function of their regulatory targets, as observed across humans, flies, and worms [139]. To date, few large comparative network studies exist, and more are needed to reveal common themes of network evolution [140]. However, mechanistic studies have added important insights to the knowledge of GRN patterns underlying evo-devo [141] and our study contributes to this active field.

Primary cilia hypothesized to underlie sexual development and the evolution of sex determination

Numerous lines of evidence from our results suggest that primary cilia may be involved not only in TSD sexual development but also in the evolution of sex determination. **First**, five of the 37 TFs that changed targets between TSD and GSD turtles (EMX2, LHX9, LIN54, ARID3B, and MEOX2) could be functionally annotated across all six networks in turtles and showed significant results in the semantic similarity tests, enabling alternative hypotheses testing. All five returned overrepresentation terms for primary cilia, sensory organelles [32] known to be involved in mammalian urogenital development [142–144]. Our results link these organelles to turtle sexual development and to evolutionary transitions in vertebrate sex determination for the first time, to our knowledge. **Second**, our trajectory analysis identified seven other TFs (HMBOX1, HOXD3, NFIA, SMAD4, SOX10, TCF3, ZEB1) that showed significant divergence between *Chrysemys* and *Apalone*, but whose results were not comprehensive enough for hypothesis testing. Notably, these seven TFs also returned terms related to primary cilia. **Third**, several of the TFs whose regulatory functions may have been taken over at least partially by ZBED1 in *Apalone* are linked to primary cilia directly or indirectly (e.g., CTCF, GLI2, GLIS3, MTF1, NR2F6, PKNOX2, RXRA, TGIF1, ZNF410), supporting the notion that evolutionary shifts related to primary cilia accompanied the evolution of turtle sex determination. **Fourth**, ESRRG, the steroid receptor that returned functional annotations only for *Apalone,* regulates ciliary development [145].

EMX2, LHX9, LIN54, and ARID3B have known links to sexual development and reproduction, and MEOX2 arises here as candidate for this new putative role. ARID3B may have evolved by developmental systems drift because its new target genes carry out the ancestral function (hypothesis H1A), while EMX2, LHX9, LIN54, and MEOX2 may have evolved by natural selection because their new targets in *Apalone* exhibit differences in their functional annotation from the putative ancestral targets in *Chrysemys* (hypothesis H1B). No evidence was found that the ancestral role of EMX2, LHX9, LIN54, and MEOX2 (i.e., the functions they orchestrate) might have been adopted by another TF (hypothesis H2). Only ARID3B

returned primary cilia related terms in both species (Cpi-MPT and Asp-M26 networks), while the primary cilia terms for the other four TFs were found exclusively in *Apalone* networks: all four *Apalone* networks for EMX2 and MEOX2, while solely Asp-M26 for LHX9 and LIN54. This association with male development at cooler temperatures suggests that there may be important sex- or species-specific patterns associated with this organelle, a hypothesis that requires future validation. We now discuss each of these five TFs separately.

Emx2 is involved in the formation of cilia [146] which help transduce Wnt signals important for gonadogenesis [74–77], a process EMX2 also mediates in mammals. Our results show EMX2 was more divergent and returned fewer overrepresented terms for Asp-M31 (a network lacking strong primary cilia terms) than for all other networks (where primary cilia terms were strongly present), pointing to a potentially reduced EMX2 functionality in Asp-M31, which we hypothesize may prevent warmer temperatures from interfering with proper sexual differentiation of *Apalone* males at ancestrally-feminizing temperatures [19]. Our results may reflect a new role acquired in *Apalone* at late stages where *Emx2* differential transcription could induce differential ciliogenesis, perhaps via natural selection in concert with the evolution of *Meox2.* Indeed, we found evidence of regulatory coevolution for EMX2 and MEOX2. These two TFs clustered tightly within each species (Fig 3D) because their targets overlapped more than any other TFs (by >70%) but also evolved substantially in parallel between *Chrysemys* and *Apalone*. This pattern could occur if they co-regulate the same genes, or if they compete for similar binding sites. This would be possible because TFs can overlap greatly in their active binding of targets yet induce different functional outcomes (via gene expression) due to the combinatorics of other aspects that fine tune regulation and influence the differential usage of shared binding sites [147].

The observed coevolution of *Emx2* and *Meox2* is intriguing because our results would expand the putative roles for ***Meox2***. *Meox2*'s thermosensitive and male-specific expression in turtles [19] combined with its close association with EMX2, a known sexual development gene, render *Meox2* a novel candidate for a role in turtle sexual development whose evolution between *Chrysemys* and *Apalone* may have contributed to transitions in sex determination. MEOX2 returned different biological process terms between turtle species, suggesting a role shift for this TF may have occurred. As this shift implicates the primary cilia, it could affect the thermosensory machinery, a notion supported by the *Drosophila* homologue of MEOX2, *btn,* which mediates responses to noxious temperature [95]. Furthermore, within species, calcium channel terms were overrepresented for MEOX2 at Cpi-MPT but not Cpi-FPT networks, tying this TF to an important known component of epigenetic regulation of TSD gonadal development [21,22]. And intriguingly, *Meox2* represses transcriptional co-activation by β-catenin [95] a key ovarian development gene in TSD turtles [148].

Lhx9, another vertebrate gonadal development gene [76,77,79–82] appears to have shifted between our focal TSD and GSD turtles in its location in the regulatory network and in the function of its protein targets, from channels and plasma membrane associated with calcium channels in *Chrysemys*, to nucleus, cytoplasm, and cytoskeleton but not calcium channel terms in *Apalone*. This divergence is of interest because calcium signaling plays an important role in TSD turtles like *Trachemys* [21], and the cytoskeleton affects primary cilia formation and maintenance [84] among other functions. Indeed, *Lhx9* appears prone to developmental shifts despite its putatively critical role in the establishment of the gonad. In *Trachemys*, *Lhx9* is expressed throughout the thermosensitive period but upregulated only in males at stage 15 [20], although it is also present in stage 26 ovaries [149]. Meanwhile, in *Chrysemys*, *Lhx9* is upregulated in males throughout the thermosensitive period. Finally, in *Apalone*, *Lhx9* is upregulated in females or in females developing at ancestrally feminizing (warm) temperature [19]. Such developmental systems drift affects other sexual development genes across turtles and vertebrates [9,24,25].

***Lin54*,** a core subunit of the DREAM/LINC complex which is highly conserved across animals and plants [86,88–91] functions as an activator and repressor by targeting different gene sets [86] and plays roles in development, reproduction in invertebrates [86,87] and perhaps mammals [86] where a paralog of *Lin54*, *Mtl5*, has testis-specific action during spermatocyte meiosis [88]. Interestingly, LIN54 favors binding to autosomes in the soma and influences the X chromosome gene expression indirectly in *C. elegans* [86], where it helps DNA repair [91]. In turtles, we observed significantly

overrepresented terms related to development for LIN54 targets in *Chrysemys*, and to primary cilia in *Apalone.* But because LIN54 is related to Wnt signaling (sensed with the help of primary cilia), which is important for gonadogenesis in TSD and GSD turtles [150,151] and other vertebrates [1], our results render *Lin54* an interesting candidate ever-present and primed to help transduce differential Wnt signaling during sexual development.

Arid3b is expressed in numerous cancer types including breast and ovarian cancer [72,152–154] perhaps because it regulates the cell cycle and stem cell genes [152] as it is a member of the LIN28-let-7-ARID3B pathway that promotes cell proliferation [73]. While not itself a member of the DREAM complex, ARID3B binds to E2F and RB family genes [152] which are important members of the DREAM complex [88], and along with LIN54, regulate the mitotic gene *Cdc2* [89,152]. ARID3B is also expressed in the Leydig cells [72], and binds to *Wnt1* [73]. Importantly, our results showed that ARID3B was most differential between *Chrysemys* networks, where it targets genes related to channel activity and membrane transport at Cpi-FPT in agreement with the reported regulation of TSD female development via the phosphorylation of STAT3 mediated by calcium channels, which represses *Kdm6b* expression and consequently, the epigenetic activation of *Dmrt1* and downstream male-differentiation genes [22]. Our observations render ARID3B an important upstream candidate for male and female development in *Chrysemys* with putative opposite action to MEOX2 which exhibited overrepresentation of calcium channel terms at Cpi-MPT but not Cpi-FPT networks in this TSD turtle.

Evolution of *Dhh*, a known candidate gene, is also linked to the turnover in sex determination associated to primary cilia

We previously identified *Dhh* (Desert Hedgehog Signaling Molecule) as a gene with sex-specific expression that switched between *Chrysemys* and *Apalone* [19]. *Dhh* is upregulated at FPT (31°C) during the thermosensitive period in *Chrysemys*, and in males or at 26°C in *Apalone* at the same stages (15–22) [19]. In contrast, *Dhh* was not expressed during a similar time window in *Trachemys* (stages 15–19 and 21) [20]. *Dhh* is involved in mammalian testis development and upregulated in male mice during stages e11.6-e12.0 which correspond to turtle stages 18–21 [20,155,156]. *Apalone's* transcriptional pattern agrees with mammalian *Dhh* expression and its role in testis development, suggesting an evolutionary shift between *Apalone* and *Chrysemys* lineages in *Dhh* regulation. Our qualitative results suggest that the TFs NFIA and CTCF may have increased their targeting of *Dhh* in *Chrysemys* relative to *Apalone*, and 17 other TFs may have increased targeting of *Dhh* in *Apalone* relative to *Chrysemys,* including LHX9, MEOX2, EMX2, and ARID3B related to primary cilia, plus BARHL2, LHX2, ISL2, ALX1, HESX1, LHX8, ELF5, HIF1A, HEY2, MNT, VAX1, BHLHE40, and MSX1 (implicated in female pathways via active male downregulation [1]).

Hedgehog signaling is dependent on primary cilia in vertebrates, better characterized for hedgehog genes *Shh* and *Ihh* [157], but also *Dhh* [158]. Specifically, hedgehog signaling components were found in primary cilia of immature Leydig cells [158,159], whose differentiation is induced by DHH signaling, thus rendering DHH signaling via primary cilia a potential regulator of Leydig cell recruitment and or differentiation [158–160]. DHH signaling is also present in mouse ovary shortly after birth where it participates in theca cell differentiation [161], pointing to a general role in specification of steroidogenic cells in the gonad. Furthermore, a direct link between DHH signaling and primary cilia via a Type II non-canonical cilia signaling mechanism was detected in the developing mouse heart [162].

Novel *Primary Cilia Integration* hypothesis extends the calcium and redox (CaRe) sex determination model

Primary cilia are antennae-like organelles, now recognized as essential for the perception and transduction of signals in most cell types, whose disfunction is linked to numerous diseases, including hypogonadism and genitourinary disorders of development (reviewed in [32]). The primary cilium consists of a basal body made up of the centriole (which moonlights as the mitotic spindle), a transition zone (the cilium gateway), and an axoneme typically made up of nine microtubule doublets [32,74]. Proteins are moved up and down the axoneme via anterograde (IFT-A, kinesin) and retrograde (IFT-B, dynein) transport. The ciliary membrane can contain numerous proteins including TRP channels, which are important for

relaying Ca^{2+}, to communicate environmental changes such as temperature, mechanical force, and other signals, and is key to the primary cilia's ability to integrate environmental inputs to the cell [163–165]. Primary cilia are also involved in relaying numerous signaling pathways beyond hedgehog and Wnt, including GPCR, TGF-B/BMP, NF-kB, among several others [32,157,166–169]. Thus, primary cilia are uniquely suited to integrate environmental cues into developmental outputs, such as is essential for developmental plasticity.

Our findings suggest a link between primary cilia and turtle sexual development, expanding previous reports showing they play a critical role in the development of the urogenital ridge [142], Wolffian ducts (mediated by DHH signaling) [143], and somatic and germline gonadal components in mammals [142,144] and perhaps also in *Paralichthys olivaceus*, a fish with a thermosensitive XY system [170]. Namely, TFs with overrepresented terms related to the primary cilia present in *Chrysemys* and *Apalone*, include ARID3B, EMX2, LHX9, LIN54, and MEOX2 described above, plus DLX2, HIC2, HMBOX1, HOXD3, LHX2, MSX1, NFIA, SHOX, SHOX2, SMAD4, SOX10, and ZEB1, of which LHX2 [115,116], MSX1 [118–120], SMAD4 [121], and SOX10 [122] have known ties to gonadal development. Because primary cilia are organelles found in nearly all vertebrate cell types that help cells understand the context of cues from the environment or signaling pathways, including Wnt signaling [171] and hedgehog signaling [157], here we propose a new testable hypothesis based on our results and basic primary cilia biology, that integrates and expands upon the calcium and redox (CaRe) model of sex determination [21]. The CaRe model posits that thermosensitive cytoplasmic calcium and mitochondrial redox signaling interactions activate or repress male- and female-specific developmental pathways [21]. And we note that importantly, primary cilia are linked to both reactive oxygen species (ROS) and calcium signaling.

Our *Primary Cilia Integration* hypothesis (Fig 4) proposes that primary cilia might be important antennae relaying environmental cues and integrating them via the signaling pathways they mediate [32,163–165] to help guide sex determination and differentiation in TSD turtles. Warmer temperatures would mediate calcium signaling through TRP channels present in ciliary membranes [163,164,172] and TRP genes are already implicated in TSD biology [21,22,85]. Calcium fluxes through TRP channels that open at warmer temperature induce the documented phosphorylation of STAT3 which is demonstrated to inhibit *Kdm6b* expression in TSD turtles, thus favoring female developmental pathways [9,22,173]. Additionally primary cilia are known in other vertebrates to transduce Wnt signaling [83,168,174], hedgehog signaling [143,158,162], NF-kB signaling [169], and are negatively regulated by NRF2 signaling [175,176], all pathways with reported links to sex determination [21]. Wnt's and hedgehog's signaling role in vertebrate gonadal development is well documented: (a) Wnt canonical signaling is linked to female development [77,148,150,177], increases under female producing temperatures in the snapping turtle *Chelydra serpentina* [150], and failure to inhibit it in humans disrupts male development [178]; (b) hedgehog canonical signaling is linked to male development and is entirely dependent on the primary cilium [143,157–159]; and (c) Wnt and hedgehog signaling can be mutually antagonistic [179] consistent with the mutual inhibition required for alterative commitment to male or female developmental fate [1]. NRF2, a TF overrepresented in our study, is important for germ cell proliferation, survival, and spermatogenesis in vertebrates by combating mitochondrial ROS in gonads [180,181]. HSF2, a TF differentially expressed in turtles [Gessler et al. 2023] and involved in vertebrate spermatogenesis [182], interacts with HSF1 during heat shock and oxidative stress response in vertebrates [183,184]. And the TF NF-kB, which is differentially transcribed in turtles [19,78], also participates in vertebrate gonadal differentiation [185,186]. Research is warranted to determine the cells and developmental stages when specific steps or components of this model take place or are active, in order to functionally validate, rule out, or modify this hypothesis.

The PCI expanded model reveals several new questions to guide future studies in turtles, and multiple aspects of the model must be functionally validated, such as exploring the thermosensitivity of hedgehog, identifying the agent which phosphorylates STAT3, and characterizing the makeup of primary cilia membranes. The evolutionary changes revealed by our analyses as described earlier suggest that important modifications might have occurred at several levels in *Apalone* compared to *Chrysemys*, including in the rate of ciliogenesis, in the morphology and composition of the primary cilia, and in the location of ciliary proteins (ciliary versus extraciliary) which can affect their functions (altering cell cycle regulation,

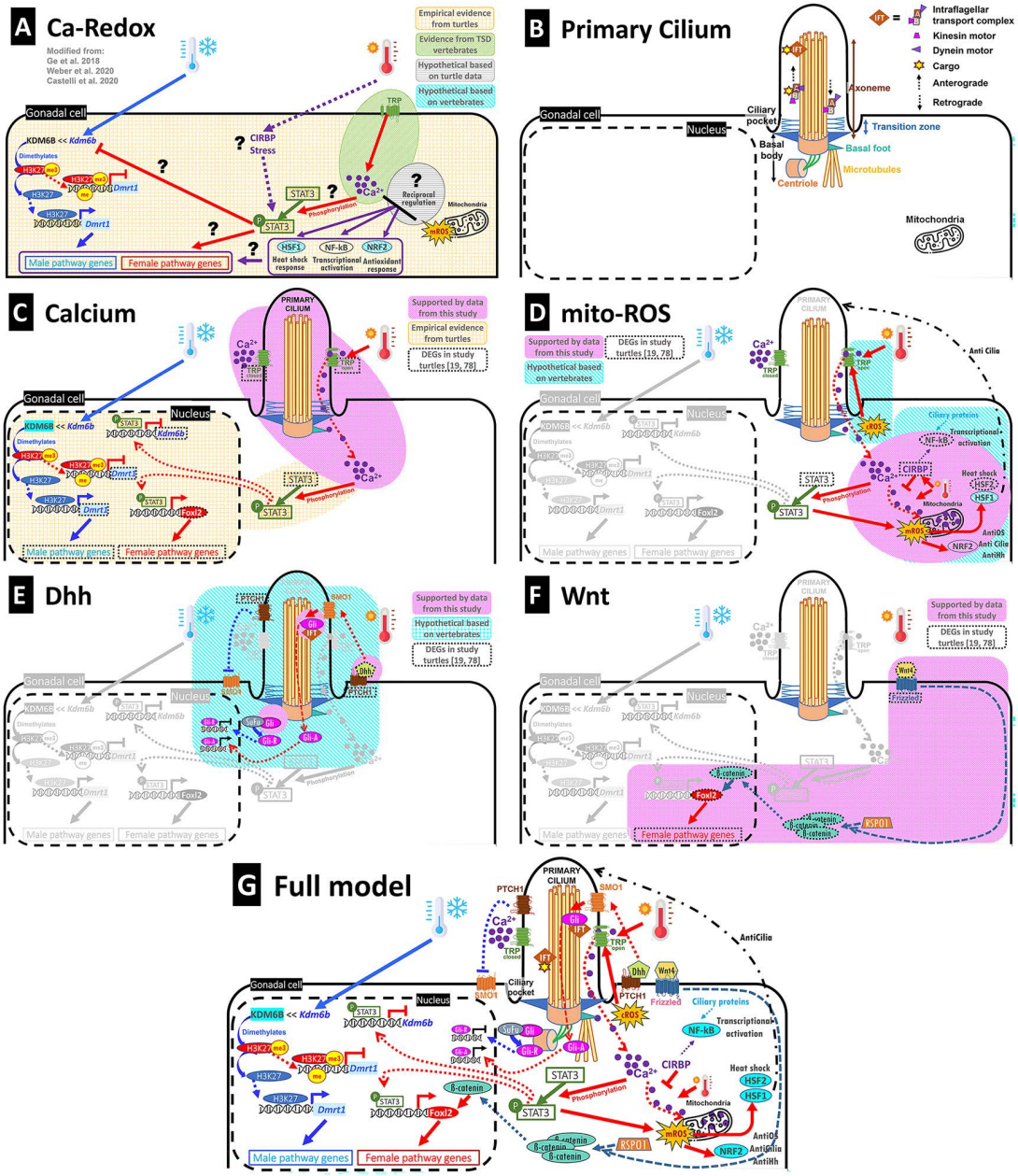


Fig 4. ***Primary cilia integration (PCI)*** **hypothesis of temperature-dependent sex determination and differentiation.** This hypothetical model is informed by findings in this study from *Chrysemys picta* and *Apalone spinifera* and from literature on other TSD turtles, and TSD and GSD vertebrates (see text for further details). Some components of this working model may be cell type-specific and stage-specific, and some may have pleiotropic effects in other functions and tissues that do not invalidate their potential participation in turtle sexual development as hypothesized here. A) Previous Calcium-Redox model where thermosensitive calcium-redox signaling activates or represses sexual development pathways [21]. B) Primary cilium structure [32,74]. C) PCI-hypothesized calcium signaling mediated through the primary cilium with reported effect of calcium on sex determination [22]. D) PCI-hypothesized calcium signaling mediated through the primary cilium with potential cross talk to mitochondrial reactive oxygen species [187,188] and activation of known associated pathways [189,190]. E) PCI-hypothesized thermosensitive hedgehog signaling mediated through the primary cilium, of which DHH is involved in gonadal development [158–160], and our hypothesis testing results suggest this signaling pathway might be differentially regulated between *Chrysemys* and *Apalone*, including its Gli proteins component. F) Thermosensitive Wnt signaling potentially mediated by the primary cilium with known influence on sex determination pathways [74–77], whose components are differentially expressed in developing female *Chrysemys* and *Apalone* [Radhakrishnan et al. 2017; Gessler et al. 2023. G) Full *Primary Cilia Integration* model. TRP channels would open at warm temperatures, allowing Ca^{2+} influx into the primary cilium. This Ca^{2+} could be relayed to the cytosol and transported to the mitochondria, potentially contributing to the

production of reactive oxygen species (ROS), which would alter the CaRe status of the cell. At lower temperatures, TRP channels would be closed, blocking entry of Ca^{2+}. CIRBP would inhibit movement of Ca^{2+} into the mitochondria and may help modulate the CaRe state. CaRe crosstalk may influence signaling pathways like HSF1 (in which HFS2 participates [183]), NF-kB, and NRF2 [21], which have known ties to the primary cilium [189,190], of which NF-kB signaling is mediated by CIRBP [190]. Under the PCI, when high temperatures raise Ca^{2+} levels, STAT3 is phosphorylated by a still unknown factor [perhaps by JAK family kinases [191]]. In TSD turtles, pSTAT3 is known to inhibit transcription of *Kdm6b*, a histone demethylase [22]. When STAT3 is unphosphorylated at cooler temperatures, *Kdm6b* is expressed and can activate *Dmrt1* through demethylation of H3K27me3, driving expression of male pathway genes. Failure to produce KDM6B protein results in retention of silencing chromatin marks (H3K27me3) at the *Dmrt1* promoter, inhibiting expression of male pathway genes [22]. Furthermore, pSTAT3 binds to the *Foxl2* promoter, driving downstream expression of female pathway genes [173]. *Foxl2* expression may be further enhanced by the accumulation of β-catenin in response to Wnt signaling which is stabilized by RSPO1 [192]. Wnt signaling can be mediated by the primary cilium [32] and is thermosensitive in TSD turtles [193]. DHH, another signaling pathway important for sexual development and dependent on the primary cilium [158], may be temperature sensitive and evolutionarily labile [194]. When activated, DHH ligands binds to PTCH1 receptors which allows activation of SMO1, a protein that converts GLI transcription factors into active forms that can activate downstream target genes [98,162].

https://doi.org/10.1371/journal.pone.0353280.g004

cytoskeletal regulation, and trafficking) [195]. Additionally, the species-specific role of each of the candidate TFs identified here must be tested.

Another important question is how do sex chromosomes interface with the primary cilia as would be predicted if primary cilia underlie the evolution of vertebrate sex determination? This question is challenging because the sex-determining genes of turtles with sex chromosomes have not been identified, such that it is unclear whether *Apalone*'s GSD system is controlled by a dominant W factor or by the dosage of a recessive Z factor, but other sex-linked genes involved in gonadal development are known in turtles. For instance, *Wt1*, the Wilm's tumor protein 1 gene involved in the development of the bipotential gonad and later testes [196] or ovaries depending on the spliceoform [197], causes Wilm's tumors which are associated with primary cilia disfunction [198]. And intriguingly, *Wt1* is linked to the sex chromosomes in *Glyptemys insculpta* and *Siebenrockiella crassicollis* turtles, two species with independently evolved XY systems [199]. Likewise, *Dmrt1*, a testis development gene tied to testicular germ cell cancer which is also associated with primary cilia disfunction [200], is linked to the sex chromosomes of *Staurotypus triporcatus* turtles, another lineage with an independently evolved XY system [199]. Further, the steroidogenic factor 1 gene *Sf1*, a target and partner of *Wt1* during gonadal development [192], is tied to metabolic homeostasis [201] that primary cilia mediate [202], and is linked to the ZW sex chromosomes of *Apalone spinifera* softshell turtles [203]. Emerging resources, such as the development of turtle organoids [204], will provide an excellent functional genomics resource in which to investigate the potential role of primary cilia in sensing the environment during gonadal sex determination and differentiation for TSD species. Indeed, previous studies have examined the effects of primary cilia in mammary organoids [105,109].

Conclusions

We generated gene-transcription factor sexual development networks for two turtle species, *Chrysemys picta* and *Apalone spinifera*. While generalized in scope due to sample pooling, the characteristics of these networks are consistent with previously reported biology of sexual development. These networks represent mechanistic hypothesis to inform future investigations into the evolution of sex determination in turtles and vertebrates. Our results support the following conclusions that can drive future targeted research efforts: (1) There may be a large degree of conservation in transcription factor hubs between *Chrysemys* and *Apalone*, consistent with the prevailing understanding of a high degree of conservation in elements of vertebrate sex determination networks and evo-devo toolkit hypotheses, but that warrant further research with larger sampling to rule out the alternative that differences exist in these components that pass undetected in our study. (2) While the TF hubs appeared conserved, the targets of shared hubs often were not. In some cases, these varying targets converged on similar functional annotations, suggesting a role for developmental systems drift. In other cases, target genes significantly differed in their functional annotations suggesting a possibility of natural selection or genetic drift to be at play. (3) We identified one TF with conserved targets (perhaps ancestral) that may have undergone

developmental systems drift to target additional genes targets during GSD evolution or alternatively, an example of a dozen TFs that may have converged in TSD to regulate the targets of the conserved TF. (4) Several candidate TFs were detected that are of interest as they have known roles in mammalian sexual development and our analysis expands their role to sex determination in reptiles. (5) Qualitative results identified predicted regulatory changes in *Dhh* that could underpin its male-to-female shift in gene expression previously observed between *Apalone* and *Chrysemys*. (6) Finally, our findings suggest that primary cilia might be tightly linked to sexual development in both TSD and GSD species. Thus, we propose a potential role for primary cilia as the sentinels of environmental signaling in TSD, explicitly linking them to this function while expanding upon the CaRe Hypothesis, and tying them to transitions in sex determination for the first time. Given the ability of the primary cilium to interface with the environment and with so many signaling pathways (several with known ties to sexual development), it is tempting to hypothesize that they could underly the evolutionary diversity observed in vertebrate sex determination more broadly.

Further research is warranted to test these hypotheses, including comparative proteomics of primary cilia in developing gonads of TSD and GSD species to elucidate finer details of their compositional dynamics during cell differentiation at various embryonic stages of sexual development. This approach is still missing both in our general understanding of primary cilia function and in their role in development and disease [32], but will also help decipher the role of primary cilia in the molecular and cellular evolution of plasticity and canalization.

Supporting information

S1 File. Supporting Information.
(ZIP)

Acknowledgments

We thank Parnal Joshi for help in preparing the protein-protein interaction dataset used in the generation of the networks. We thank Leila Fattel for analytical suggestions in our functional annotation. We note that ChatGPT was used to help brainstorm some R commands in order to streamline code generation, and any resulting code was then tested and fine-tuned by TBG for validation to ensure it achieved the appropriate aim. Thus, all scripts have been validated and are fully available and functional.

Author contributions

Conceptualization: Thea B. Gessler, Nicole Valenzuela.

Data curation: Thea B. Gessler.

Formal analysis: Thea B. Gessler, Dean C. Adams.

Funding acquisition: Nicole Valenzuela.

Investigation: Thea B. Gessler.

Methodology: Thea B. Gessler, Dean C. Adams.

Project administration: Thea B. Gessler, Nicole Valenzuela.

Resources: Nicole Valenzuela.

Supervision: Nicole Valenzuela.

Visualization: Thea B. Gessler, Nicole Valenzuela.

Writing – original draft: Thea B. Gessler, Nicole Valenzuela.

Writing – review & editing: Thea B. Gessler, Dean C. Adams, Nicole Valenzuela.

References

1. Capel B. Vertebrate sex determination: evolutionary plasticity of a fundamental switch. Nat Rev Genet. 2017;18(11):675–89. https://doi.org/10.1038/nrg.2017.60 PMID: 28804140
2. Morrish BC, Sinclair AH. Vertebrate sex determination: many means to an end. Reproduction. 2002;124(4):447–57. https://doi.org/10.1530/rep.0.1240447 PMID: 12361462
3. Bachtrog D, Mank JE, Peichel CL, Kirkpatrick M, Otto SP, Ashman T-L, et al. Sex determination: why so many ways of doing it? PLoS Biol. 2014;12(7):e1001899. https://doi.org/10.1371/journal.pbio.1001899 PMID: 24983465
4. Stöck M, Kratochvíl L, Kuhl H, Rovatsos M, Evans BJ, Suh A, et al. A brief review of vertebrate sex evolution with a pledge for integrative research: towards "sexomics". Philos Trans R Soc Lond B Biol Sci. 2021;376(1832):20200426. https://doi.org/10.1098/rstb.2020.0426 PMID: 34247497
5. True JR, Haag ES. Developmental system drift and flexibility in evolutionary trajectories. Evol Dev. 2001;3(2):109–19. https://doi.org/10.1046/j.1525-142x.2001.003002109.x PMID: 11341673
6. Valenzuela N. Sexual Development and the Evolution of Sex Determination. Sex Dev. 2008;2(2):64–72. https://doi.org/10.1159/000129691
7. Tree of Sex Consortium. Tree of Sex: a database of sexual systems. Sci Data. 2014;1:140015. https://doi.org/10.1038/sdata.2014.15 PMID: 25977773
8. Smith CA, Roeszler KN, Ohnesorg T, Cummins DM, Farlie PG, Doran TJ, et al. The avian Z-linked gene DMRT1 is required for male sex determination in the chicken. Nature. 2009;461(7261):267–71. https://doi.org/10.1038/nature08298 PMID: 19710650
9. Ge C, Ye J, Zhang H, Zhang Y, Sun W, Sang Y, et al. Dmrt1 induces the male pathway in a turtle species with temperature-dependent sex determination. Development. 2017;144(12):2222–33. https://doi.org/10.1242/dev.152033 PMID: 28506988
10. Cui Z, Liu Y, Wang W, Wang Q, Zhang N, Lin F, et al. Genome editing reveals dmrt1 as an essential male sex-determining gene in Chinese tongue sole (Cynoglossus semilaevis). Sci Rep. 2017;7:42213. https://doi.org/10.1038/srep42213 PMID: 28205594
11. Morais da Silva S, Hacker A, Harley V, Goodfellow P, Swain A, Lovell-Badge R. Sox9 expression during gonadal development implies a conserved role for the gene in testis differentiation in mammals and birds. Nat Genet. 1996;14(1):62–8. https://doi.org/10.1038/ng0996-62 PMID: 8782821
12. Navarro-Martín L, Viñas J, Ribas L, Díaz N, Gutiérrez A, Di Croce L, et al. DNA methylation of the gonadal aromatase (cyp19a) promoter is involved in temperature-dependent sex ratio shifts in the European sea bass. PLoS Genet. 2011;7(12):e1002447. https://doi.org/10.1371/journal.pgen.1002447 PMID: 22242011
13. Tree of Sex Consortium. Tree of Sex: a database of sexual systems. Sci Data. 2014;1:140015. https://doi.org/10.1038/sdata.2014.15 PMID: 25977773
14. Valenzuela N, Adams DC. Chromosome number and sex determination coevolve in turtles. Evolution. 2011;65(6):1808–13. https://doi.org/10.1111/j.1558-5646.2011.01258.x PMID: 21644965
15. Literman R, Burrett A, Bista B, Valenzuela N. Putative Independent Evolutionary Reversals from Genotypic to Temperature-Dependent Sex Determination are Associated with Accelerated Evolution of Sex-Determining Genes in Turtles. J Mol Evol. 2018;86(1):11–26. https://doi.org/10.1007/s00239-017-9820-x PMID: 29192334
16. Bista B, Valenzuela N. Turtle Insights into the Evolution of the Reptilian Karyotype and the Genomic Architecture of Sex Determination. Genes (Basel). 2020;11(4):416. https://doi.org/10.3390/genes11040416 PMID: 32290488
17. Valenzuela N. Evolution of the gene network underlying gonadogenesis in turtles with temperature-dependent and genotypic sex determination. Integr Comp Biol. 2008;48(4):476–85. https://doi.org/10.1093/icb/icn031 PMID: 21669808
18. Badenhorst D, Hillier LW, Literman R, Montiel EE, Radhakrishnan S, Shen Y, et al. Physical Mapping and Refinement of the Painted Turtle Genome (Chrysemys picta) Inform Amniote Genome Evolution and Challenge Turtle-Bird Chromosomal Conservation. Genome Biol Evol. 2015;7(7):2038–50. https://doi.org/10.1093/gbe/evv119 PMID: 26108489
19. Gessler TB, Wu Z, Valenzuela N. Transcriptomic thermal plasticity underlying gonadal development in a turtle with ZZ/ZW sex chromosomes despite canalized genotypic sex determination. Ecol Evol. 2023;13(2):e9854. https://doi.org/10.1002/ece3.9854 PMID: 36844670
20. Czerwinski M, Natarajan A, Barske L, Looger LL, Capel B. A timecourse analysis of systemic and gonadal effects of temperature on sexual development of the red-eared slider turtle Trachemys scripta elegans. Dev Biol. 2016;420(1):166–77. https://doi.org/10.1016/j.ydbio.2016.09.018 PMID: 27671871
21. Castelli M, Whiteley S, Georges A, Holleley C. Cellular calcium and redox regulation: the mediator of vertebrate environmental sex determination? Biological Reviews. 2020;95(3). https://doi.org/10.1111/brv.12582
22. Weber C, Zhou Y, Lee JG, Looger LL, Qian G, Ge C, et al. Temperature-dependent sex determination is mediated by pSTAT3 repression of Kdm6b. Science. 2020;368(6488):303–6. https://doi.org/10.1126/science.aaz4165 PMID: 32299951
23. Sun W, Cai H, Zhang G, Zhang H, Bao H, Wang L, et al. Dmrt1 is required for primary male sexual differentiation in Chinese soft-shelled turtle Pelodiscus sinensis. Sci Rep. 2017;7(1):4433. https://doi.org/10.1038/s41598-017-04938-5 PMID: 28667307
24. Valenzuela N, Neuwald JL, Literman R. Transcriptional evolution underlying vertebrate sexual development. Dev Dyn. 2013;242(4):307–19. https://doi.org/10.1002/dvdy.23897 PMID: 23108853
25. Mizoguchi B, Valenzuela N. Alternative splicing and thermosensitive expression of Dmrt1 during urogenital development in the painted turtle, Chrysemys picta. PeerJ. 2020;8:e8639. https://doi.org/10.7717/peerj.8639 PMID: 32219017

26. Carroll SB. Evo-devo and an expanding evolutionary synthesis: a genetic theory of morphological evolution. Cell. 2008;134(1):25–36. https://doi.org/10.1016/j.cell.2008.06.030 PMID: 18614008
27. Williams TM, Carroll SB. Genetic and molecular insights into the development and evolution of sexual dimorphism. Nat Rev Genet. 2009;10(11):797–804. https://doi.org/10.1038/nrg2687 PMID: 19834484
28. Helsen J, Frickel J, Jelier R, Verstrepen KJ. Network hubs affect evolvability. PLoS Biol. 2019;17(1):e3000111. https://doi.org/10.1371/journal.pbio.3000111 PMID: 30699103
29. Koubkova-Yu TC-T, Chao J-C, Leu J-Y. Heterologous Hsp90 promotes phenotypic diversity through network evolution. PLoS Biol. 2018;16(11):e2006450. https://doi.org/10.1371/journal.pbio.2006450 PMID: 30439936
30. Badenhorst D, Stanyon R, Engstrom T, Valenzuela N. A ZZ/ZW microchromosome system in the spiny softshell turtle, Apalone spinifera, reveals an intriguing sex chromosome conservation in Trionychidae. Chromosome Res. 2013;21(2):137–47. https://doi.org/10.1007/s10577-013-9343-2 PMID: 23512312
31. Sabath N, Itescu Y, Feldman A, Meiri S, Mayrose I, Valenzuela N. Sex determination, longevity, and the birth and death of reptilian species. Ecol Evol. 2016;6(15):5207–20. https://doi.org/10.1002/ece3.2277 PMID: 27551377
32. Mill P, Christensen ST, Pedersen LB. Primary cilia as dynamic and diverse signalling hubs in development and disease. Nat Rev Genet. 2023;24(7):421–41. https://doi.org/10.1038/s41576-023-00587-9 PMID: 37072495
33. Glass K, Huttenhower C, Quackenbush J, Yuan G-C. Passing messages between biological networks to refine predicted interactions. PLoS One. 2013;8(5):e64832. https://doi.org/10.1371/journal.pone.0064832 PMID: 23741402
34. Schlauch D, Paulson JN, Young A, Glass K, Quackenbush J. Estimating gene regulatory networks with pandaR. Bioinformatics. 2017;33(14):2232–4. https://doi.org/10.1093/bioinformatics/btx139 PMID: 28334344
35. Valenzuela N. Egg incubation and collection of painted turtle embryos. Cold Spring Harb Protoc. 2009;2009(7):pdb.prot5238. https://doi.org/10.1101/pdb.prot5238 PMID: 20147203
36. Yntema CL. A series of stages in the embryonic development of Chelydra serpentina. J Morphol. 1968;125(2):219–51. https://doi.org/10.1002/jmor.1051250207 PMID: 5681661
37. Greenbaum E, Carr JL. Staging criteria for embryos of the spiny softshell turtle, Apalone spinifera (Testudines: Trionychidae). J Morphol. 2002;254(3):272–91. https://doi.org/10.1002/jmor.10036 PMID: 12386898
38. Cordero GA, Janzen FJ. An enhanced developmental staging table for the painted turtle, Chrysemys picta (ATestudines: Emydidae). J Morphol. 2014;275(4):442–55. https://doi.org/10.1002/jmor.20226 PMID: 24301536
39. Valenzuela N. Constant, Shift, and Natural Temperature Effects on Sex Determination in Podocnemis expansa Turtles. Ecology. 2001;82(11):3010. https://doi.org/10.2307/2679831
40. Gómez-Saldarriaga C, Valenzuela N, Ceballos CP. Effects of Incubation Temperature on Sex Determination in the Endangered Magdalena River Turtle,Podocnemis lewyana. Chelonian Conservation and Biology. 2016;15(1):43–53. https://doi.org/10.2744/ccb-1170.1
41. Yao HH-C, DiNapoli L, Capel B. Cellular mechanisms of sex determination in the red-eared slider turtle, Trachemys scripta. Mech Dev. 2004;121(11):1393–401. https://doi.org/10.1016/j.mod.2004.06.001 PMID: 15454268
42. Greenbaum E, Carr JL. Sexual differentiation in the spiny softshell turtle (Apalone spinifera), a species with genetic sex determination. J Exp Zool. 2001;290(2):190–200. https://doi.org/10.1002/jez.1049 PMID: 11471149
43. Literman R, Radhakrishnan S, Tamplin J, Burke R, Dresser C, Valenzuela N. Development of sexing primers in Glyptemys insculpta and Apalone spinifera turtles uncovers an XX/XY sex-determining system in the critically-endangered bog turtle Glyptemys muhlenbergii. Conservation Genet Resour. 2017;9(4):651–8. https://doi.org/10.1007/s12686-017-0711-7
44. Literman R, Badenhorst D, Valenzuela N. qPCR-based molecular sexing by copy number variation in rRNA genes and its utility for sex identification in soft-shell turtles. Methods Ecol Evol. 2014;5(9):872–80. https://doi.org/10.1111/2041-210x.12228
45. Bolger AM, Lohse M, Usadel B. Trimmomatic: a flexible trimmer for Illumina sequence data. Bioinformatics. 2014;30(15):2114–20. https://doi.org/10.1093/bioinformatics/btu170 PMID: 24695404
46. Wu TD, Watanabe CK. GMAP: a genomic mapping and alignment program for mRNA and EST sequences. Bioinformatics. 2005;21(9):1859–75. https://doi.org/10.1093/bioinformatics/bti310 PMID: 15728110
47. Wu TD, Nacu S. Fast and SNP-tolerant detection of complex variants and splicing in short reads. Bioinformatics. 2010;26(7):873–81. https://doi.org/10.1093/bioinformatics/btq057 PMID: 20147302
48. Bista B, González-Rodelas L, Álvarez-González L, Wu Z q, Montiel EE, Lee LS. De novo genome assemblies of two cryptodiran turtles with ZZ/ZW and XX/XY sex chromosomes provide insights into patterns of genome reshuffling and uncover novel 3D genome folding in amniotes. Genome Research. 2024;34:1553–69. https://doi.org/10.1101/gr.279443.124
49. Pertea M, Pertea GM, Antonescu CM, Chang T-C, Mendell JT, Salzberg SL. StringTie enables improved reconstruction of a transcriptome from RNA-seq reads. Nat Biotechnol. 2015;33(3):290–5. https://doi.org/10.1038/nbt.3122 PMID: 25690850
50. Soneson C, Love MI, Robinson MD. Differential analyses for RNA-seq: transcript-level estimates improve gene-level inferences. F1000Res. 2015;4:1521. https://doi.org/10.12688/f1000research.7563.2 PMID: 26925227

51. Robinson MD, McCarthy DJ, Smyth GK. edgeR: a Bioconductor package for differential expression analysis of digital gene expression data. Bioinformatics. 2010;26(1):139–40. https://doi.org/10.1093/bioinformatics/btp616 PMID: 19910308
52. Nitta KR, Jolma A, Yin Y, Morgunova E, Kivioja T, Akhtar J, et al. Conservation of transcription factor binding specificities across 600 million years of bilateria evolution. Elife. 2015;4:e04837. https://doi.org/10.7554/eLife.04837 PMID: 25779349
53. Schmidt D, Wilson MD, Ballester B, Schwalie PC, Brown GD, Marshall A, et al. Five-vertebrate ChIP-seq reveals the evolutionary dynamics of transcription factor binding. Science. 2010;328(5981):1036–40. https://doi.org/10.1126/science.1186176 PMID: 20378774
54. Lowry JA, Atchley WR. Molecular evolution of the GATA family of transcription factors: conservation within the DNA-binding domain. J Mol Evol. 2000;50(2):103–15. https://doi.org/10.1007/s002399910012 PMID: 10684344
55. Fornes O, Castro-Mondragon JA, Khan A, Robin, Zhang X, Richmond PA, et al. JASPAR 2020: update of the open-access database of transcription factor binding profiles. Nucleic Acids Research. 2019. https://doi.org/10.1093/nar/gkz1001
56. Gearing LJ, Cumming HE, Chapman R, Finkel AM, Woodhouse IB, Luu K, et al. CiiiDER: A tool for predicting and analysing transcription factor binding sites. PLoS One. 2019;14(9):e0215495. https://doi.org/10.1371/journal.pone.0215495 PMID: 31483836
57. Aptekmann AA, Bulavka D, Nadra AD, Sánchez IE. Transcription factor specificity limits the number of DNA-binding motifs. PLoS One. 2022;17(1):e0263307. https://doi.org/10.1371/journal.pone.0263307 PMID: 35089985
58. Krieger G, Lupo O, Wittkopp P, Barkai N. Evolution of transcription factor binding through sequence variations and turnover of binding sites. Genome Res. 2022;32(6):1099–111. https://doi.org/10.1101/gr.276715.122 PMID: 35618416
59. Rao S, Ahmad K, Ramachandran S. Cooperative binding between distant transcription factors is a hallmark of active enhancers. Mol Cell. 2021;81(8):1651–1665.e4. https://doi.org/10.1016/j.molcel.2021.02.014 PMID: 33705711
60. Tuğrul M, Paixão T, Barton NH, Tkačik G. Dynamics of Transcription Factor Binding Site Evolution. PLoS Genet. 2015;11(11):e1005639. https://doi.org/10.1371/journal.pgen.1005639 PMID: 26545200
61. Szklarczyk D, Gable AL, Lyon D, Junge A, Wyder S, Huerta-Cepas J, et al. STRING v11: protein-protein association networks with increased coverage, supporting functional discovery in genome-wide experimental datasets. Nucleic Acids Res. 2019;47(D1):D607–13. https://doi.org/10.1093/nar/gky1131 PMID: 30476243
62. Glass K, Quackenbush J, Silverman EK, Celli B, Rennard SI, Yuan G-C, et al. Sexually-dimorphic targeting of functionally-related genes in COPD. BMC Syst Biol. 2014;8:118. https://doi.org/10.1186/s12918-014-0118-y PMID: 25431000
63. Glass K, Quackenbush J, Spentzos D, Haibe-Kains B, Yuan G-C. A network model for angiogenesis in ovarian cancer. BMC Bioinformatics. 2015;16:115. https://doi.org/10.1186/s12859-015-0551-y PMID: 25888305
64. Adams DC, Collyer ML. A general framework for the analysis of phenotypic trajectories in evolutionary studies. Evolution. 2009;63(5):1143–54. https://doi.org/10.1111/j.1558-5646.2009.00649.x PMID: 19210539
65. Thomas PD, Ebert D, Muruganujan A, Mushayahama T, Albou L-P, Mi H. PANTHER: Making genome-scale phylogenetics accessible to all. Protein Sci. 2022;31(1):8–22. https://doi.org/10.1002/pro.4218 PMID: 34717010
66. Mi H, Muruganujan A, Huang X, Ebert D, Mills C, Guo X, et al. Protocol Update for large-scale genome and gene function analysis with the PANTHER classification system (v.14.0). Nat Protoc. 2019;14(3):703–21. https://doi.org/10.1038/s41596-019-0128-8 PMID: 30804569
67. Mi H, Thomas P. PANTHER Pathway: An Ontology-Based Pathway Database Coupled with Data Analysis Tools. Humana Press. 2009.
68. Ziemann M, Schroeter B, Bora A. Two subtle problems with overrepresentation analysis. Bioinform Adv. 2024;4(1):vbae159. https://doi.org/10.1093/bioadv/vbae159 PMID: 39539946
69. Zhao K, Rhee SY. Interpreting omics data with pathway enrichment analysis. Trends Genet. 2023;39(4):308–19. https://doi.org/10.1016/j.tig.2023.01.003 PMID: 36750393
70. Zhao C, Wang Z. GOGO: An improved algorithm to measure the semantic similarity between gene ontology terms. Sci Rep. 2018;8(1):15107. https://doi.org/10.1038/s41598-018-33219-y PMID: 30305653
71. Shannon P, Markiel A, Ozier O, Baliga NS, Wang JT, Ramage D, et al. Cytoscape: a software environment for integrated models of biomolecular interaction networks. Genome Res. 2003;13(11):2498–504. https://doi.org/10.1101/gr.1239303 PMID: 14597658
72. Samyesudhas SJ, Roy L, Cowden Dahl KD. Differential expression of ARID3B in normal adult tissue and carcinomas. Gene. 2014;543(1):174–80. https://doi.org/10.1016/j.gene.2014.04.007 PMID: 24704276
73. Ali A, Anthony RV, Bouma GJ, Winger QA. LIN28-let-7 axis regulates genes in immortalized human trophoblast cells by targeting the ARID3B-complex. FASEB J. 2019;33(11):12348–63. https://doi.org/10.1096/fj.201900718RR PMID: 31415216
74. Long X, Chen L, Xiao X, Min X, Wu Y, Yang Z, et al. Structure, function, and research progress of primary cilia in reproductive physiology and reproductive diseases. Front Cell Dev Biol. 2024;12:1418928. https://doi.org/10.3389/fcell.2024.1418928 PMID: 38887518
75. Miyamoto N, Yoshida M, Kuratani S, Matsuo I, Aizawa S. Defects of urogenital development in mice lacking Emx2. Development. 1997;124(9):1653–64. https://doi.org/10.1242/dev.124.9.1653 PMID: 9165114
76. Knarston IM, Pachernegg S, Robevska G, Ghobrial I, Er PX, Georges E, et al. An In Vitro Differentiation Protocol for Human Embryonic Bipotential Gonad and Testis Cell Development. Stem Cell Reports. 2020;15(6):1377–91. https://doi.org/10.1016/j.stemcr.2020.10.009
77. Wilhelm D, Perea-Gomez A, Newton A, Chaboissier M-C. Gonadal sex determination in vertebrates: rethinking established mechanisms. Development. 2025;152(6):dev204592. https://doi.org/10.1242/dev.204592 PMID: 40162719

78. Radhakrishnan S, Literman R, Neuwald J, Severin A, Valenzuela N. Transcriptomic responses to environmental temperature by turtles with temperature-dependent and genotypic sex determination assessed by RNAseq inform the genetic architecture of embryonic gonadal development. PLoS One. 2017;12(3):e0172044. https://doi.org/10.1371/journal.pone.0172044 PMID: 28296881

79. Bieser KL, Wibbels T. Chronology, magnitude and duration of expression of putative sex-determining/differentiation genes in a turtle with temperature-dependent sex determination. Sex Dev. 2014;8(6):364–75. https://doi.org/10.1159/000369116 PMID: 25427533

80. Birk OS, Casiano DE, Wassif CA, Cogliati T, Zhao L, Zhao Y, et al. The LIM homeobox gene Lhx9 is essential for mouse gonad formation. Nature. 2000;403(6772):909–13. https://doi.org/10.1038/35002622 PMID: 10706291

81. Garcia-Alonso L, Lorenzi V, Mazzeo CI, Alves-Lopes JP, Roberts K, Sancho-Serra C, et al. Single-cell roadmap of human gonadal development. Nature. 2022;607(7919):540–7. https://doi.org/10.1038/s41586-022-04918-4 PMID: 35794482

82. Lei L, Chen C, Zhu J, Wang Y, Liu X, Liu H, et al. Transcriptome analysis reveals key genes and pathways related to sex differentiation in the Chinese soft-shelled turtle (Pelodiscus sinensis). Comp Biochem Physiol Part D Genomics Proteomics. 2022;42:100986. https://doi.org/10.1016/j.cbd.2022.100986 PMID: 35447559

83. May-Simera HL, Kelley MW. Cilia, Wnt signaling, and the cytoskeleton. Cilia. 2012;1(1):7. https://doi.org/10.1186/2046-2530-1-7 PMID: 23351924

84. Ge R, Cao M, Chen M, Liu M, Xie S. Cytoskeletal networks in primary cilia: Current knowledge and perspectives. J Cell Physiol. 2022;237(11):3975–83. https://doi.org/10.1002/jcp.30865 PMID: 36000703

85. Yatsu R, Miyagawa S, Kohno S, Saito S, Lowers RH, Ogino Y, et al. TRPV4 associates environmental temperature and sex determination in the American alligator. Sci Rep. 2015;5:18581. https://doi.org/10.1038/srep18581 PMID: 26677944

86. Tabuchi TM, Deplancke B, Osato N, Zhu LJ, Barrasa MI, Harrison MM, et al. Chromosome-biased binding and gene regulation by the Caenorhabditis elegans DRM complex. PLoS Genet. 2011;7(5):e1002074. https://doi.org/10.1371/journal.pgen.1002074 PMID: 21589891

87. Cheng M-H, Andrejka L, Vorster PJ, Hinman A, Lipsick JS. The Drosophila LIN54 homolog Mip120 controls two aspects of oogenesis. Biol Open. 2017;6(7):967–78. https://doi.org/10.1242/bio.025825 PMID: 28522430

88. Hoareau M, Rincheval-Arnold A, Gaumer S, Guénal I. DREAM a little dREAM of DRM: Model organisms and conservation of DREAM-like complexes. BioEssays. 2023;46(2). https://doi.org/10.1002/bies.202300125

89. Schmit F, Cremer S, Gaubatz S. LIN54 is an essential core subunit of the DREAM/LINC complex that binds to the cdc2 promoter in a sequence-specific manner. FEBS J. 2009;276(19):5703–16. https://doi.org/10.1111/j.1742-4658.2009.07261.x PMID: 19725879

90. Marceau AH, Felthousen JG, Goetsch PD, Iness AN, Lee H-W, Tripathi SM, et al. Structural basis for LIN54 recognition of CHR elements in cell cycle-regulated promoters. Nat Commun. 2016;7:12301. https://doi.org/10.1038/ncomms12301 PMID: 27465258

91. Bujarrabal-Dueso A, Sendtner G, Meyer DH, Chatzinikolaou G, Stratigi K, Garinis GA, et al. The DREAM complex functions as conserved master regulator of somatic DNA-repair capacities. Nat Struct Mol Biol. 2023;30(4):475–88. https://doi.org/10.1038/s41594-023-00942-8 PMID: 36959262

92. Candia AF, Hu J, Crosby J, Lalley PA, Noden D, Nadeau JH, et al. Mox-1 and Mox-2 define a novel homeobox gene subfamily and are differentially expressed during early mesodermal patterning in mouse embryos. Development. 1992;116(4):1123–36. https://doi.org/10.1242/dev.116.4.1123 PMID: 1363541

93. Candia AF, Wright CV. Differential localization of Mox-1 and Mox-2 proteins indicates distinct roles during development. Int J Dev Biol. 1996;40(6):1179–84. https://doi.org/10.1387/ijdb.9032023 PMID: 9032023

94. Reijntjes S, Stricker S, Mankoo BS. A comparative analysis of Meox1 and Meox2 in the developing somites and limbs of the chick embryo. Int J Dev Biol. 2007;51(8):753–9. https://doi.org/10.1387/ijdb.072332sr PMID: 17939123

95. Kokotović T, Lenartowicz EM, Langeslag M, Ciotu CI, Fell CW, Scaramuzza A, et al. Transcription factor mesenchyme homeobox protein 2 (MEOX2) modulates nociceptor function. FEBS J. 2022;289(12):3457–76. https://doi.org/10.1111/febs.16347 PMID: 35029322

96. Ye Y-Z, Li J, Li W, Fu X, Zhang J, Yang S, et al. Transcriptional control of male-specific pathway in temperature-dependent sex determination. Sci Bull (Beijing). 2025. https://doi.org/10.1016/j.scib.2025.07.025 PMID: 40883156

97. Hilgendorf KI, Johnson CT, Mezger A, Rice SL, Norris AM, Demeter J, et al. Omega-3 Fatty Acids Activate Ciliary FFAR4 to Control Adipogenesis. Cell. 2019;179(6):1289–1305.e21. https://doi.org/10.1016/j.cell.2019.11.005 PMID: 31761534

98. Kim J, Kato M, Beachy PA. Gli2 trafficking links Hedgehog-dependent activation of Smoothened in the primary cilium to transcriptional activation in the nucleus. Proc Natl Acad Sci U S A. 2009;106(51):21666–71. https://doi.org/10.1073/pnas.0912180106 PMID: 19996169

99. Hsiao C-J, Chang C-H, Ibrahim RB, Lin I-H, Wang C-H, Wang W-J, et al. Gli2 modulates cell cycle re-entry through autophagy-mediated regulation of the length of primary cilia. J Cell Sci. 2018;131(24):jcs221218. https://doi.org/10.1242/jcs.221218 PMID: 30463852

100. Jetten AM, Scoville DW, Kang HS. GLIS1-3: Links to Primary Cilium, Reprogramming, Stem Cell Renewal, and Disease. Cells. 2022;11(11):1833. https://doi.org/10.3390/cells11111833

101. Kang HS, Beak JY, Kim Y-S, Herbert R, Jetten AM. Glis3 is associated with primary cilia and Wwtr1/TAZ and implicated in polycystic kidney disease. Mol Cell Biol. 2009;29(10):2556–69. https://doi.org/10.1128/MCB.01620-08 PMID: 19273592

102. Chung M-I, Peyrot SM, LeBoeuf S, Park TJ, McGary KL, Marcotte EM, et al. RFX2 is broadly required for ciliogenesis during vertebrate development. Dev Biol. 2012;363(1):155–65. https://doi.org/10.1016/j.ydbio.2011.12.029 PMID: 22227339

103. Ashique AM, Choe Y, Karlen M, May SR, Phamluong K, Solloway MJ, et al. The Rfx4 transcription factor modulates Shh signaling by regional control of ciliogenesis. Sci Signal. 2009;2(95):ra70. https://doi.org/10.1126/scisignal.2000602 PMID: 19887680

104. Pillai-Kastoori L, Wen W, Wilson SG, Strachan E, Lo-Castro A, Fichera M, et al. Sox11 is required to maintain proper levels of Hedgehog signaling during vertebrate ocular morphogenesis. PLoS Genet. 2014;10(7):e1004491. https://doi.org/10.1371/journal.pgen.1004491 PMID: 25010521

105. McDermott KM, Liu BY, TIsty TD, Pazour GJ. Primary cilia regulate branching morphogenesis during mammary gland development. Curr Biol. 2010;20(8):731–7. https://doi.org/10.1016/j.cub.2010.02.048 PMID: 20381354

106. Anderson AE, Taniguchi K, Hao Y, Melhuish TA, Shah A, Turner SD, et al. Tgif1 and Tgif2 Repress Expression of the RabGAP Evi5l. Mol Cell Biol. 2017;37(5):e00527–16. https://doi.org/10.1128/MCB.00527-16 PMID: 27956704

107. Sarkisian MR, Siebzehnrubl D, Hoang-Minh L, Deleyrolle L, Silver DJ, Siebzehnrubl FA, et al. Detection of primary cilia in human glioblastoma. J Neurooncol. 2014;117(1):15–24. https://doi.org/10.1007/s11060-013-1340-y PMID: 24510433

108. Song T, Zhou J. Primary cilia in corneal development and disease. Zool Res. 2020;41(5):495–502. https://doi.org/10.24272/j.issn.2095-8137.2020.109 PMID: 32808517

109. Guen VJ, Chavarria TE, Kröger C, Ye X, Weinberg RA, Lees JA. EMT programs promote basal mammary stem cell and tumor-initiating cell stemness by inducing primary ciliogenesis and Hedgehog signaling. Proc Natl Acad Sci U S A. 2017;114(49):E10532–9. https://doi.org/10.1073/pnas.1711534114 PMID: 29158396

110. Wu Y, Hu X, Li Z, Wang M, Li S, Wang X, et al. Transcription Factor RFX2 Is a Key Regulator of Mouse Spermiogenesis. Sci Rep. 2016;6:20435. https://doi.org/10.1038/srep20435 PMID: 26853561

111. VanWert JM, Wolfe SA, Grimes SR. Binding of RFX2 and NF-Y to the testis-specific histone H1t promoter may be required for transcriptional activation in primary spermatocytes. J Cell Biochem. 2008;104(3):1087–101. https://doi.org/10.1002/jcb.21694 PMID: 18247329

112. Kistler WS, Baas D, Lemeille S, Paschaki M, Seguin-Estevez Q, Barras E, et al. RFX2 Is a Major Transcriptional Regulator of Spermiogenesis. PLoS Genet. 2015;11(7):e1005368. https://doi.org/10.1371/journal.pgen.1005368 PMID: 26162102

113. Pellegrini M, Pantano S, Lucchini F, Fumi M, Forabosco A. Emx2 developmental expression in the primordia of the reproductive and excretory systems. Anat Embryol (Berl). 1997;196(6):427–33. https://doi.org/10.1007/s004290050110 PMID: 9453363

114. Daftary GS, Taylor HS. EMX2 gene expression in the female reproductive tract and aberrant expression in the endometrium of patients with endometriosis. J Clin Endocrinol Metab. 2004;89(5):2390–6. https://doi.org/10.1210/jc.2003-031389 PMID: 15126568

115. Singh N, Singh D, Bhide A, Sharma R, Sahoo S, Jolly MK, et al. Lhx2 in germ cells suppresses endothelial cell migration in the developing ovary. Exp Cell Res. 2022;415(1):113108. https://doi.org/10.1016/j.yexcr.2022.113108 PMID: 35337816

116. Singh N, Singh D, Bhide A, Sharma R, Bhowmick S, Patel V, et al. LHX2 in germ cells control tubular organization in the developing mouse testis. Exp Cell Res. 2023;425(1):113511. https://doi.org/10.1016/j.yexcr.2023.113511 PMID: 36796745

117. Mazaud S, Oréal E, Guigon CJ, Carré-Eusèbe D, Magre S. Lhx9 expression during gonadal morphogenesis as related to the state of cell differentiation. Gene Expr Patterns. 2002;2(3–4):373–7. https://doi.org/10.1016/s1567-133x(02)00050-9 PMID: 12617828

118. Le Bouffant R, Souquet B, Duval N, Duquenne C, Hervé R, Frydman N, et al. Msx1 and Msx2 promote meiosis initiation. Development. 2011;138(24):5393–402. https://doi.org/10.1242/dev.068452 PMID: 22071108

119. Xie H, Cherrington BD, Meadows JD, Witham EA, Mellon PL. Msx1 homeodomain protein represses the αGSU and GnRH receptor genes during gonadotrope development. Mol Endocrinol. 2013;27(3):422–36. https://doi.org/10.1210/me.2012-1289 PMID: 23371388

120. Sun J, Ting M-C, Ishii M, Maxson R. Msx1 and Msx2 function together in the regulation of primordial germ cell migration in the mouse. Dev Biol. 2016;417(1):11–24. https://doi.org/10.1016/j.ydbio.2016.07.013 PMID: 27435625

121. Itman C, Loveland KL. SMAD expression in the testis: An insight into BMP regulation of spermatogenesis. Developmental Dynamics. 2008;237(1):97–111. https://doi.org/10.1002/dvdy.21401

122. Polanco JC, Wilhelm D, Davidson T-L, Knight D, Koopman P. Sox10 gain-of-function causes XX sex reversal in mice: implications for human 22q-linked disorders of sex development. Hum Mol Genet. 2010;19(3):506–16. https://doi.org/10.1093/hmg/ddp520 PMID: 19933217

123. Valenzuela N, LeClere A, Shikano T. Comparative gene expression of steroidogenic factor 1 in Chrysemys picta and Apalone mutica turtles with temperature-dependent and genotypic sex determination. Evol Dev. 2006;8(5):424–32. https://doi.org/10.1111/j.1525-142X.2006.00116.x PMID: 16925678

124. Valenzuela N, Shikano T. Embryological ontogeny of aromatase gene expression in Chrysemys picta and Apalone mutica turtles: comparative patterns within and across temperature-dependent and genotypic sex-determining mechanisms. Dev Genes Evol. 2007;217(1):55–62. https://doi.org/10.1007/s00427-006-0106-3 PMID: 17021865

125. Valenzuela N. Relic thermosensitive gene expression in a turtle with genotypic sex determination. Evolution. 2008;62(1):234–40. https://doi.org/10.1111/j.1558-5646.2007.00279.x PMID: 18053078

126. Valenzuela N. Multivariate expression analysis of the gene network underlying sexual development in turtle embryos with temperature-dependent and genotypic sex determination. Sex Dev. 2010;4(1–2):39–49. https://doi.org/10.1159/000277935 PMID: 20110645

127. Rivero-Hinojosa S, Pugacheva EM, Kang S, Méndez-Catalá CF, Kovalchuk AL, Strunnikov AV, et al. The combined action of CTCF and its testis-specific paralog BORIS is essential for spermatogenesis. Nat Commun. 2021;12(1):3846. https://doi.org/10.1038/s41467-021-24140-6 PMID: 34158481

128. Kitamura Y, Takahashi K, Maezawa S, Munakata Y, Sakashita A, Katz SP, et al. CTCF-mediated 3D chromatin sets up the gene expression program in the male germline. Nat Struct Mol Biol. 2025;32(7):1227–40. https://doi.org/10.1038/s41594-025-01482-z PMID: 40033153

129. Bischof JM, Gillen AE, Song L, Gosalia N, London D, Furey TS, et al. A genome-wide analysis of open chromatin in human epididymis epithelial cells reveals candidate regulatory elements for genes coordinating epididymal function. Biol Reprod. 2013;89(4):104. https://doi.org/10.1095/biolreprod.113.110403 PMID: 24006278

130. Browne JA, Yang R, Song L, Crawford GE, Leir S-H, Harris A. Open chromatin mapping identifies transcriptional networks regulating human epididymis epithelial function. Mol Hum Reprod. 2014;20(12):1198–207. https://doi.org/10.1093/molehr/gau075 PMID: 25180270

131. Wu C, Ding X, Li H, Zhu C, Xiong C. Genome-wide promoter methylation profile of human testis and epididymis: identified from cell-free seminal DNA. BMC Genomics. 2013;14:288. https://doi.org/10.1186/1471-2164-14-288 PMID: 23622456

132. Baddela VS, Sharma A, Michaelis M, Vanselow J. HIF1 driven transcriptional activity regulates steroidogenesis and proliferation of bovine granulosa cells. Sci Rep. 2020;10(1):3906. https://doi.org/10.1038/s41598-020-60935-1 PMID: 32127571

133. He Z, Yan R-G, Shang Q-B, Yang Q-E. Transcriptomic dynamics and cell-to-cell communication during the transition of prospermatogonia to spermatogonia revealed at single-cell resolution. BMC Genomics. 2025;26(1):58. https://doi.org/10.1186/s12864-025-11244-2 PMID: 39838296

134. Li S, Yan R-G, Gao X, He Z, Wu S-X, Wang Y-J, et al. Single-cell transcriptome analyses reveal critical regulators of spermatogonial stem cell fate transitions. BMC Genomics. 2024;25(1):138. https://doi.org/10.1186/s12864-024-10072-0 PMID: 38310206

135. Singh N, Singh D, Modi D. LIM Homeodomain (LIM-HD) Genes and Their Co-Regulators in Developing Reproductive System and Disorders of Sex Development. Sex Dev. 2022;16(2–3):147–61. https://doi.org/10.1159/000518323 PMID: 34518474

136. Choi Y, Ballow DJ, Xin Y, Rajkovic A. Lim homeobox gene, lhx8, is essential for mouse oocyte differentiation and survival. Biol Reprod. 2008;79(3):442–9. https://doi.org/10.1095/biolreprod.108.069393 PMID: 18509161

137. Crews D, Bull JJ. Mode and tempo in environmental sex determination in vertebrates. Semin Cell Dev Biol. 2009;20(3):251–5. https://doi.org/10.1016/j.semcdb.2009.02.004 PMID: 19429496

138. Bista B, Wu Z, Literman R, Valenzuela N. Thermosensitive sex chromosome dosage compensation in ZZ/ZW softshell turtles, Apalone spinifera. Philos Trans R Soc Lond B Biol Sci. 2021;376(1833):20200101. https://doi.org/10.1098/rstb.2020.0101 PMID: 34304598

139. Boyle AP, Araya CL, Brdlik C, Cayting P, Cheng C, Cheng Y, et al. Comparative analysis of regulatory information and circuits across distant species. Nature. 2014;512(7515):453–6. https://doi.org/10.1038/nature13668 PMID: 25164757

140. Karasawa T, Koshikawa S. Evolution of gene regulatory networks in insects. Curr Opin Insect Sci. 2025;69:101365. https://doi.org/10.1016/j.cois.2025.101365 PMID: 40348447

141. Van Belleghem SM, Ruggieri AA, Concha C, Livraghi L, Hebberecht L, Rivera ES, et al. High level of novelty under the hood of convergent evolution. Science. 2023;379(6636):1043–9. https://doi.org/10.1126/science.ade0004 PMID: 36893249

142. Wainwright EN, Svingen T, Ng ET, Wicking C, Koopman P. Primary cilia function regulates the length of the embryonic trunk axis and urogenital field in mice. Dev Biol. 2014;395(2):342–54. https://doi.org/10.1016/j.ydbio.2014.08.037 PMID: 25224227

143. Alves MBR, Girardet L, Augière C, Moon KH, Lavoie-Ouellet C, Bernet A, et al. Hedgehog signaling regulates Wolffian duct development through the primary cilium†. Biol Reprod. 2023;108(2):241–57. https://doi.org/10.1093/biolre/ioac210 PMID: 36525341

144. Piprek RP, Podkowa D, Kloc M, Kubiak JZ. Expression of primary cilia-related genes in developing mouse gonads. Int J Dev Biol. 2019;63(11–12):615–21. https://doi.org/10.1387/ijdb.190049rp PMID: 32149371

145. Wesselman HM, Flores-Mireles AL, Bauer A, Pei L, Wingert RA. Esrrγa regulates nephron and ciliary development by controlling prostaglandin synthesis. Development. 2023;150(10):dev201411. https://doi.org/10.1242/dev.201411 PMID: 37232416

146. Nguyen TK, Rodriguez J-M, Wesselman HM, Wingert RA. Emx2 is an essential regulator of ciliated cell development across embryonic tissues. iScience. 2024;27(12):111271. https://doi.org/10.1016/j.isci.2024.111271 PMID: 39687012

147. Holub AS, Choudury SG, Andrianova EP, Dresden CE, Camacho RU, Zhulin IB, et al. START domains generate paralog-specific regulons from a single network architecture. Nat Commun. 2024;15(1):9861. https://doi.org/10.1038/s41467-024-54269-z PMID: 39543118

148. Mork L, Capel B. Conserved action of β-catenin during female fate determination in the red-eared slider turtle. Evol Dev. 2013;15(2):96–106. https://doi.org/10.1111/ede.12020 PMID: 25098635

149. Barske LA, Capel B. Estrogen represses SOX9 during sex determination in the red-eared slider turtle Trachemys scripta. Dev Biol. 2010;341(1):305–14. https://doi.org/10.1016/j.ydbio.2010.02.010 PMID: 20153744

150. Rhen T, Even Z, Brenner A, Lodewyk A, Das D, Singh S, et al. Evolutionary Turnover in Wnt Gene Expression but Conservation of Wnt Signaling during Ovary Determination in a TSD Reptile. Sex Dev. 2021;15(1–3):47–68. https://doi.org/10.1159/000516973 PMID: 34280932

151. Zhou T, Zhang H, Chen M, Zhang Y, Chen G, Zou G, et al. Identification and Expression Analysis of Wnt2 Gene in the Sex Differentiation of the Chinese Soft-Shelled Turtle (Pelodiscus sinensis). Life (Basel). 2023;13(1):188. https://doi.org/10.3390/life13010188 PMID: 36676139

152. Saadat K, Lestari W, Pratama E, Ma T, Iseki S, Tatsumi M, et al. Distinct and overlapping roles of ARID3A and ARID3B in regulating E2F-dependent transcription via direct binding to E2F target genes. International Journal of Oncology. 2021;58(4). https://doi.org/10.3892/ijo.2021.5192

153. Bobbs A, Gellerman K, Hallas WM, Joseph S, Yang C, Kurkewich J, et al. ARID3B Directly Regulates Ovarian Cancer Promoting Genes. PLoS One. 2015;10(6):e0131961. https://doi.org/10.1371/journal.pone.0131961 PMID: 26121572

154. Oguz Erdogan AS, Ozdemirler N, Oyken M, Alper M, Erson-Bensan AE. ARID3B expression in primary breast cancers and breast cancer-derived cell lines. Cell Oncol (Dordr). 2014;37(4):289–96. https://doi.org/10.1007/s13402-014-0185-5 PMID: 25120063

155. Munger SC, Natarajan A, Looger LL, Ohler U, Capel B. Fine time course expression analysis identifies cascades of activation and repression and maps a putative regulator of mammalian sex determination. PLoS Genetics. 2013;9(7):e1003630. https://doi.org/10.1371/journal.pgen.1003630

156. Pachernegg S, Georges E, Ayers K. The Desert Hedgehog Signalling Pathway in Human Gonadal Development and Differences of Sex Development. Sex Dev. 2022;16(2–3):98–111. https://doi.org/10.1159/000518308 PMID: 34518472

157. Bangs F, Anderson KV. Primary Cilia and Mammalian Hedgehog Signaling. Cold Spring Harb Perspect Biol. 2017;9(5):a028175. https://doi.org/10.1101/cshperspect.a028175 PMID: 27881449

158. Nygaard MB, Almstrup K, Lindbæk L, Christensen ST, Svingen T. Cell context-specific expression of primary cilia in the human testis and ciliary coordination of Hedgehog signalling in mouse Leydig cells. Sci Rep. 2015;5:10364. https://doi.org/10.1038/srep10364 PMID: 25992706

159. Yao HH-C, Whoriskey W, Capel B. Desert Hedgehog/Patched 1 signaling specifies fetal Leydig cell fate in testis organogenesis. Genes Dev. 2002;16(11):1433–40. https://doi.org/10.1101/gad.981202 PMID: 12050120

160. Barsoum IB, Bingham NC, Parker KL, Jorgensen JS, Yao HH-C. Activation of the Hedgehog pathway in the mouse fetal ovary leads to ectopic appearance of fetal Leydig cells and female pseudohermaphroditism. Dev Biol. 2009;329(1):96–103. https://doi.org/10.1016/j.ydbio.2009.02.025 PMID: 19268447

161. Liu C, Peng J, Matzuk MM, Yao HH-C. Lineage specification of ovarian theca cells requires multicellular interactions via oocyte and granulosa cells. Nat Commun. 2015;6:6934. https://doi.org/10.1038/ncomms7934 PMID: 25917826

162. Fulmer D, Toomer KA, Glover J, Guo L, Moore K, Moore R, et al. Desert hedgehog-primary cilia cross talk shapes mitral valve tissue by organizing smooth muscle actin. Dev Biol. 2020;463(1):26–38. https://doi.org/10.1016/j.ydbio.2020.03.003 PMID: 32151560

163. DeCaen PG, Delling M, Vien TN, Clapham DE. Direct recording and molecular identification of the calcium channel of primary cilia. Nature. 2013;504(7479):315–8. https://doi.org/10.1038/nature12832 PMID: 24336289

164. Delling M, DeCaen PG, Doerner JF, Febvay S, Clapham DE. Primary cilia are specialized calcium signalling organelles. Nature. 2013;504(7479):311–4. https://doi.org/10.1038/nature12833 PMID: 24336288

165. Nauli SM, Pala R, Kleene SJ. Calcium channels in primary cilia. Curr Opin Nephrol Hypertens. 2016;25(5):452–8. https://doi.org/10.1097/MNH.0000000000000251 PMID: 27341444

166. Anvarian Z, Mykytyn K, Mukhopadhyay S, Pedersen LB, Christensen ST. Cellular signalling by primary cilia in development, organ function and disease. Nat Rev Nephrol. 2019;15(4):199–219. https://doi.org/10.1038/s41581-019-0116-9 PMID: 30733609

167. Jiang JY, Falcone JL, Curci S, Hofer AM. Direct visualization of cAMP signaling in primary cilia reveals up-regulation of ciliary GPCR activity following Hedgehog activation. Proc Natl Acad Sci U S A. 2019;116(24):12066–71. https://doi.org/10.1073/pnas.1819730116 PMID: 31142652

168. Lee KH. Involvement of Wnt signaling in primary cilia assembly and disassembly. FEBS J. 2020;287(23):5027–38. https://doi.org/10.1111/febs.15579 PMID: 33015954

169. Wann AKT, Chapple JP, Knight MM. The primary cilium influences interleukin-1β-induced NFκB signalling by regulating IKK activity. Cell Signal. 2014;26(8):1735–42. https://doi.org/10.1016/j.cellsig.2014.04.004 PMID: 24726893

170. Wang L, Wu Z, Zou C, Liang S, Zou Y, Liu Y, et al. Sex-Dependent RNA Editing and N6-adenosine RNA Methylation Profiling in the Gonads of a Fish, the Olive Flounder (Paralichthys olivaceus). Front Cell Dev Biol. 2020;8:751. https://doi.org/10.3389/fcell.2020.00751 PMID: 32850855

171. Lee JH, Gleeson JG. The role of primary cilia in neuronal function. Neurobiol Dis. 2010;38(2):167–72. https://doi.org/10.1016/j.nbd.2009.12.022 PMID: 20097287

172. Köttgen M, Buchholz B, Garcia-Gonzalez MA, Kotsis F, Fu X, Doerken M, et al. TRPP2 and TRPV4 form a polymodal sensory channel complex. J Cell Biol. 2008;182(3):437–47. https://doi.org/10.1083/jcb.200805124 PMID: 18695040

173. Wu P, Wang X, Ge C, Jin L, Ding Z, Liu F, et al. pSTAT3 activation of Foxl2 initiates the female pathway underlying temperature-dependent sex determination. Proc Natl Acad Sci U S A. 2024;121(37):e2401752121. https://doi.org/10.1073/pnas.2401752121 PMID: 39226347

174. Oh EC, Katsanis N. Context-dependent regulation of Wnt signaling through the primary cilium. J Am Soc Nephrol. 2013;24(1):10–8. https://doi.org/10.1681/ASN.2012050526 PMID: 23123400

175. Liu P, Dodson M, Fang D, Chapman E, Zhang DD. NRF2 negatively regulates primary ciliogenesis and hedgehog signaling. PLoS Biol. 2020;18(2):e3000620. https://doi.org/10.1371/journal.pbio.3000620 PMID: 32053600

176. Morleo M, Vieira HLA, Pennekamp P, Palma A, Bento-Lopes L, Omran H, et al. Crosstalk between cilia and autophagy: implication for human diseases. Autophagy. 2023;19(1):24–43. https://doi.org/10.1080/15548627.2022.2067383 PMID: 35613303

177. Yao HH-C. The pathway to femaleness: current knowledge on embryonic development of the ovary. Mol Cell Endocrinol. 2005;230(1–2):87–93. https://doi.org/10.1016/j.mce.2004.11.003 PMID: 15664455

178. Lundgaard Riis M, Delpouve G, Nielsen JE, Melau C, Langhoff Thuesen L, Juul Hare K, et al. Inhibition of WNT/β-catenin signalling during sex-specific gonadal differentiation is essential for normal human fetal testis development. Cell Commun Signal. 2024;22(1):330. https://doi.org/10.1186/s12964-024-01704-9 PMID: 38879537

179. Ding M, Wang X. Antagonism between Hedgehog and Wnt signaling pathways regulates tumorigenicity. Oncol Lett. 2017;14(6):6327–33. https://doi.org/10.3892/ol.2017.7030 PMID: 29391876

180. Alnajem A, Al-Maghrebi M. The Regulatory Effects of JAK2/STAT3 on Spermatogenesis and the Redox Keap1/Nrf2 Axis in an Animal Model of Testicular Ischemia Reperfusion Injury. Cells. 2023;12(18):2292. https://doi.org/10.3390/cells12182292 PMID: 37759514

181. Niu Y-J, Yuan G, Ren W, Wu J, Liu G, Zou M, et al. NRF2 deficiency impairs proliferation and survival of chicken primordial germ cells via oxidative stress, mitochondrial dysfunction and apoptosis. Poult Sci. 2026;105(6):106765. https://doi.org/10.1016/j.psj.2026.106765 PMID: 41850075

182. Gupta N, Sarkar S, Mehta P, Sankhwar SN, Rajender S. Polymorphisms in the HSF2, LRRC6, MEIG1 and PTIP genes correlate with sperm motility in idiopathic infertility. Andrologia. 2022;54(9):e14517. https://doi.org/10.1111/and.14517 PMID: 35768906

183. He H, Soncin F, Grammatikakis N, Li Y, Siganou A, Gong J, et al. Elevated expression of heat shock factor (HSF) 2A stimulates HSF1-induced transcription during stress. J Biol Chem. 2003;278(37):35465–75. https://doi.org/10.1074/jbc.M304663200 PMID: 12813038

184. Hästbacka HSE, Da Silva AJ, Sistonen L, Henriksson E. A guide to heat shock factors as multifunctional transcriptional regulators. FEBS J. 2025;292(16):4133–55. https://doi.org/10.1111/febs.70139 PMID: 40457168

185. Hong CY, Park JH, Seo KH, Kim J-M, Im SY, Lee JW, et al. Expression of MIS in the testis is downregulated by tumor necrosis factor alpha through the negative regulation of SF-1 transactivation by NF-kappa B. Mol Cell Biol. 2003;23(17):6000–12. https://doi.org/10.1128/MCB.23.17.6000-6012.2003 PMID: 12917325

186. Xia X-H, Liang N, Ma X-Y, Qin L, Wang S-Y, Chang Z-J. Inhibition of the NF-κB signaling pathway affects gonadal differentiation and leads to male bias in Paramisgurnus dabryanus. Theriogenology. 2023;207:82–95. https://doi.org/10.1016/j.theriogenology.2023.05.019 PMID: 37269599

187. Hasegawa S, Inagi R. Organelle Stress and Crosstalk in Kidney Disease. Kidney360. 2020;1(10):1157–64. https://doi.org/10.34067/KID.0002442020 PMID: 35368784

188. Bootman MD, Bultynck G. Fundamentals of Cellular Calcium Signaling: A Primer. Cold Spring Harb Perspect Biol. 2020;12(1):a038802. https://doi.org/10.1101/cshperspect.a038802 PMID: 31427372

189. Martin-Hurtado A, Martin-Morales R, Robledinos-Antón N, Blanco R, Palacios-Blanco I, Lastres-Becker I, et al. NRF2-dependent gene expression promotes ciliogenesis and Hedgehog signaling. Sci Rep. 2019;9(1):13896. https://doi.org/10.1038/s41598-019-50356-0 PMID: 31554934

190. Mc Fie M, Koneva L, Collins I, Coveney CR, Clube AM, Chanalaris A, et al. Ciliary proteins specify the cell inflammatory response by tuning NFκB signalling, independently of primary cilia. J Cell Sci. 2020;133(13):jcs239871. https://doi.org/10.1242/jcs.239871 PMID: 32503942

191. Sun W, Liao Y, Yi Q, Wu S, Tang L, Tong L. The Mechanism of CIRP in Regulation of STAT3 Phosphorylation and Bag-1/S Expression Upon UVB Radiation. Photochem Photobiol. 2018;94(6):1234–9. https://doi.org/10.1111/php.12981 PMID: 29981150

192. Wilhelm D, Perea-Gomez A, Newton A, Chaboissier M-C. Gonadal sex determination in vertebrates: rethinking established mechanisms. Development. 2025;152(6):dev204592. https://doi.org/10.1242/dev.204592 PMID: 40162719

193. Shoemaker CM, Queen J, Crews D. Response of candidate sex-determining genes to changes in temperature reveals their involvement in the molecular network underlying temperature-dependent sex determination. Mol Endocrinol. 2007;21(11):2750–63. https://doi.org/10.1210/me.2007-0263 PMID: 17684113

194. Gessler TB, Wu Z, Valenzuela N. Transcriptomic thermal plasticity underlying gonadal development in a turtle with ZZ/ZW sex chromosomes despite canalized genotypic sex determination. Ecol Evol. 2023;13(2):e9854. https://doi.org/10.1002/ece3.9854 PMID: 36844670

195. Hua K, Ferland RJ. Primary cilia proteins: ciliary and extraciliary sites and functions. Cell Mol Life Sci. 2018;75(9):1521–40. https://doi.org/10.1007/s00018-017-2740-5 PMID: 29305615

196. Gao F, Maiti S, Alam N, Zhang Z, Deng JM, Behringer RR, et al. The Wilms tumor gene, Wt1, is required for Sox9 expression and maintenance of tubular architecture in the developing testis. Proc Natl Acad Sci U S A. 2006;103(32):11987–92. https://doi.org/10.1073/pnas.0600994103 PMID: 16877546

197. Gregoire EP, De Cian M-C, Migale R, Perea-Gomez A, Schaub S, Bellido-Carreras N, et al. The -KTS splice variant of WT1 is essential for ovarian determination in mice. Science. 2023;382(6670):600–6. https://doi.org/10.1126/science.add8831 PMID: 37917714

198. Kitamura E, Cowell JK, Chang C-S, Hawthorn L. Variant profiles of genes mapping to chromosome 16q loss in Wilms tumors reveals link to cilia-related genes and pathways. Genes Cancer. 2020;11(3–4):137–53. https://doi.org/10.18632/genesandcancer.207 PMID: 33488951

199. Montiel EE, Badenhorst D, Lee LS, Literman R, Trifonov V, Valenzuela N. Cytogenetic Insights into the Evolution of Chromosomes and Sex Determination Reveal Striking Homology of Turtle Sex Chromosomes to Amphibian Autosomes. Cytogenet Genome Res. 2016;148(4):292–304. https://doi.org/10.1159/000447478 PMID: 27423490

200. Litchfield K, Levy M, Dudakia D, Proszek P, Shipley C, Basten S, et al. Rare disruptive mutations in ciliary function genes contribute to testicular cancer susceptibility. Nat Commun. 2016;7:13840. https://doi.org/10.1038/ncomms13840 PMID: 27996046

201. Dhillon H, Zigman JM, Ye C, Lee CE, McGovern RA, Tang V, et al. Leptin directly activates SF1 neurons in the VMH, and this action by leptin is required for normal body-weight homeostasis. Neuron. 2006;49(2):191–203. https://doi.org/10.1016/j.neuron.2005.12.021 PMID: 16423694

202. Yang DJ, Hong J, Kim KW. Hypothalamic primary cilium: A hub for metabolic homeostasis. Exp Mol Med. 2021;53(7):1109–15. https://doi.org/10.1038/s12276-021-00644-5 PMID: 34211092

203. Lee L, Montiel EE, Navarro-Domínguez BM, Valenzuela N. Chromosomal Rearrangements during Turtle Evolution Altered the Synteny of Genes Involved in Vertebrate Sex Determination. Cytogenet Genome Res. 2019;157(1–2):77–88. https://doi.org/10.1159/000497302 PMID: 30808820

204. Zdyrski C, Gabriel V, Gessler TB, Ralston A, Sifuentes-Romero I, Kundu D, et al. Establishment and characterization of turtle liver organoids provides a potential model to decode their unique adaptations. Commun Biol. 2024;7(1):218. https://doi.org/10.1038/s42003-024-05818-1 PMID: 38388772